Synthesis and Structural Characterization of Platinum(II) Bis(chelate) Complexes derived from the Ligand System *meso/rac*-Ph(O)HPCH$_2$CH$_2$PH(O)Ph†

John Powell,* Michael J. Horvath and Alan Lough
Department of Chemistry, University of Toronto, 80 St. George Street, Toronto, Ontario, M5S 1A1 Canada

The ligand (*R,S*)-Ph(O)HPCH$_2$CH$_2$PH(O)Ph reacted with [Pt(PPh$_3$)$_4$] to give the complex *syn*-[Pt{(*R,S*)-Ph(O)P(CH$_2$)$_2$P(OH)Ph}$_2$] **3**. In this reaction a long-lived intermediate was observed and spectroscopically characterized as the six-co-ordinate platinum(IV) *trans*-dihydride complex *syn*-[PtH$_2${(*R,S*)-Ph(O)P(CH$_2$)$_2$P(OH)Ph}$_2$] **4**. Complex **4** exhibits fluxional behaviour in CD_2Cl_2 solution at 20 °C as a result of a rapid proton exchange between the OH protons and the hydride ligand that is *syn* with respect to these groups. Mechanistic proposals were made to account for the OH proton–hydride exchange process and for the decomposition of the dihydride complex **4** to complex **3**. Treatment of **3** with dry HCl afforded the monoprotonated complex *syn*-[Pt{(*R,S*)-Ph(O)P(CH$_2$)$_2$P(OH)Ph}{(*R,S*)-Ph(OH)P(CH$_2$)$_2$P(OH)Ph}]Cl **12**. The diprotonated complex *anti*-[Pt{(*R,S*)-Ph(OH)P(CH$_2$)$_2$P(OH)Ph}$_2$]Cl$_2$ **9** was obtained by the reaction of [{PtCl$_2$(C$_2$H$_4$)}$_2$] with (*R,S*)-Ph(O)HPCH$_2$CH$_2$PH(O)Ph. Reaction of BF_3·Et$_2$O with **3** gave the macrocyclic complex *syn*-[Pt{[(*R,S*)-Ph(O)P(CH$_2$)$_2$P(O)Ph]BF$_2$}$_2$]·CH$_2$Cl$_2$ **13**. Treatment of [Pt(PPh$_3$)$_4$] with the racemic ligand (*RR,SS*)-Ph(O)HPCH$_2$CH$_2$PH(O)Ph afforded a white insoluble solid composed of the polymeric complexes *meso*-[{Pt[(*R,R*)-Ph(O)P(CH$_2$)$_2$P(OH)Ph][(*S,S*)-Ph(O)P(CH$_2$)$_2$P(OH)Ph]}$_n$] **15** and *rac*-[{Pt[(*RR,SS*)-Ph(O)P(CH$_2$)$_2$P(OH)Ph]$_2$}$_n$] **16**. Addition of HCl to this solid in CH_2Cl_2 led to the isolation of a mixture of the dicationic complexes *meso*-[Pt{(*R,R*)-Ph(OH)P(CH$_2$)$_2$P(OH)Ph}{(*S,S*)-Ph(OH)P(CH$_2$)$_2$P(OH)Ph}]Cl$_2$ **17** and *rac*-[Pt{(*RR,SS*)-Ph(OH)P(CH$_2$)$_2$P(OH)Ph}$_2$]Cl$_2$ **18**. The structures of complexes **3**, **9**, **12**, **13**, **15**, **17** and **18** have been determined by single-crystal X-ray diffraction studies.

A simple class of ditopic ligands capable of bonding to transition metals through both 'soft' phosphorus and 'hard' oxygen donor atoms and whose co-ordination chemistry is well documented are secondary phosphine oxides R$_2$P(O)H and their phosphinous acid tautomers R$_2$POH.[1] Interest in these ligands derives from their ambidentate nature which allows them to adopt a variety of metal–ligand bonding modes (types A–F).

Late transition-metal complexes containing secondary phosphinous acids (also known as hydroxyphosphines, type A) and secondary phosphinoyl ligands (type B) commonly occur. A repeatedly encountered structural form involves cisoidal disposition in a 'pseudo chelate' fashion of the ligands about a metal centre (type E). The ligand arrangement here consists formally of a phosphinoyl (R$_2$PO) and a phosphinous acid ligand (R$_2$POH) in which the hydrogen is disposed either symmetrically or unsymmetrically between the two oxygen atoms. Apart from a general interest in the co-ordination chemistry of R$_2$P(O)H–R$_2$POH ligand systems in so far as they provide the opportunity to study unusual structural types and hydrogen-bonding effects, there have been two recent reports of transition-metal catalysts incorporating R$_2$POH ligands. In 1993 Alper and Sommovigo[2] developed a palladium-based catalyst, later structurally characterized as [Pd(O$_2$PBu$^t_2$)(PBu$^t_2${OH}OPBu$^t_2$)] by Leoni *et al.*,[3] which catalyses the selective hydrogenation of the C=C bond of α,β-unsaturated carbonyl compounds very efficiently under mild conditions [10 psi (≈68.9 kPa) H$_2$, room temperature]. In 1990 van Leeuwen *et al.*[4] prepared the platinum-based hydroformylation catalyst [PtH(OPPh$_2$)(PPh$_2$OH)(PPh$_3$)] which catalyses the conversion of ethylene to propionaldehyde. However decomposition of the catalyst occurs within 24 h.

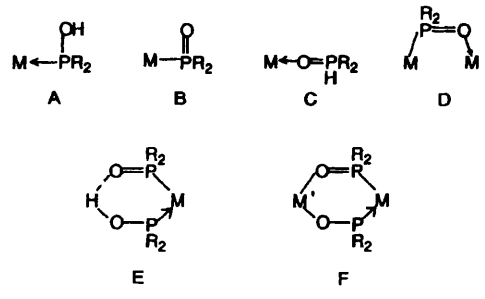

The ligating properties of phosphinous acid towards the later transition metals is limited to some degree by the fact that the free Ph$_2$P(OH) ligand rapidly equilibrates with its secondary phosphine oxide R$_2$P(O)H which is the more stable tautomeric form.[1,5] A means of overcoming this problem involves the application of the chelate effect to increase the stability of phosphinous acid complexes. Furthermore, by simple analogy with the co-ordination chemistry observed for monodentate secondary phosphine oxides, a variety of metal–ligand bonding modes should be accessible from the reactions of transition-metal complexes with multidentate secondary phosphine oxide–phosphinous acid systems (Scheme 1). However, while a variety of transition-metal complexes containing 'monodentate' R$_2$P(O)H and R$_2$P(OH) ligands are known, there is to our knowledge only one example in the literature of a metal complex containing a R(HO)P(CH$_2$)$_n$P(OH)R ligand [equation (1)], namely [NiX$_2${Ph(HO)P(CH$_2$)$_2$P(OH)Ph}$_2$] (X = Cl, Br or I) reported by Nefedov *et al.*[6]

† *Supplementary data available:* see Instructions for Authors, *J. Chem. Soc., Dalton Trans.*, 1995, Issue 1, pp. xxv–xxx.

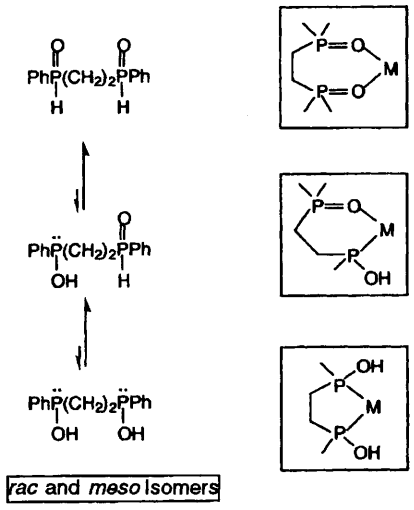

Scheme 1 Some possible co-ordination modes of the bidentate secondary phosphine oxide $Ph(O)HPCH_2CH_2PH(O)Ph$ and its tautomers

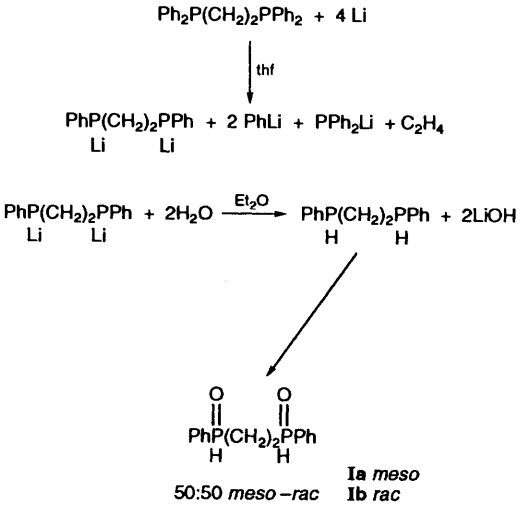

Scheme 2 Reaction sequence used for the preparation of the diastereomeric ligand mixture *meso*/*rac*-$Ph(O)HPCH_2CH_2PH(O)Ph$

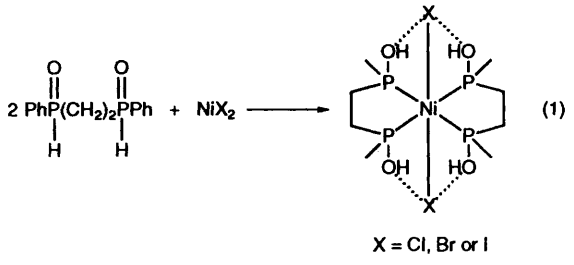

As part of a program aimed at synthesizing and delineating the co-ordination chemistry of multidentate secondary phosphine oxides and phosphinous acids we report here on the chemistry derived from the reaction of $[Pt(PPh_3)_4]$ with both *meso*- and *rac*-$Ph(O)HP(CH_2)_2PH(O)Ph$.

Results and Discussion

Ligand Synthesis.—Following an established procedure,[7] the diastereomeric mixture of the ligand 1,2-bis(hydridophenylphosphoryl)ethane was prepared in an overall yield of 40% as shown in Scheme 2. The low yield originates from an irreversible competitive side reaction in the lithiation step whereby reductive cleavage of a P–CH_2 bond leads to the formation of PPh_2Li and ethylene. While the oxidation of 1,2-bis(phenylphosphino)ethane to give 1,2-bis(hydridophenylphosphoryl)ethane was originally reported using O_2 over a period of 7 h,[7a] this transformation could be accelerated (reaction < 1 h) with no loss in efficiency by careful addition of H_2O_2 to a CH_2Cl_2 solution containing 1,2-bis(phenylphosphino)ethane. Both methods, however, afford small amounts (5%) of an impurity, which gives rise to approximately equal intensity singlet resonances at δ 27.9, 28.3, 37.3 and 37.6 in the ^{31}P-$\{^1H\}$ NMR spectrum recorded in CH_2Cl_2. A proton-coupled ^{31}P NMR spectrum shows that while the signals at δ 27.9 and 28.3 each exhibit $^1J(P–H)$ coupling of *ca.* 473 Hz, no P–H coupling is observed for the signals at δ 37.3 and 37.6. These spectroscopic data support a tentative assignment of the impurity as a (*RR*,*SS*)/(*RS*,*SR*) diastereomeric mixture of $Ph(O)HP(CH_2)_2P(O)(OH)Ph$ **II** in which only one P–H bond is present. Further characterization of this compound by mass spectrometry failed to give a parent ion at *m*/*z* 294 but exhibited a peak at 292 consistent with the proposed oxygen-bridged species **III** formed by dehydrogenation of compound **II** [equation (2)].

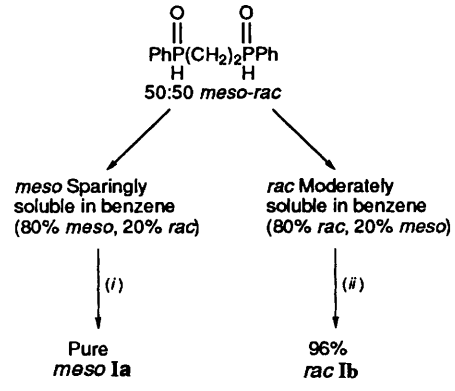

Scheme 3 Procedure for the separation and purification of the *meso* and racemic diastereomers of $Ph(O)HPCH_2CH_2PH(O)Ph$. (*i*) Recrystallized from MeOH–Et_2O; (*ii*) $SnCl_2Et_2$, CH_2Cl_2, *rac* complex soluble, *meso* complex sparingly soluble

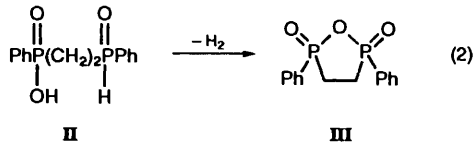

Separation and Purification of the meso *and racemic Diastereomers.*—Recrystallization of the crude diastereomeric mixture of $Ph(O)HP(CH_2)_2PH(O)Ph$ from hot benzene provided an initial crude separation of the *meso* and *rac* ligands (Scheme 3). While simple recrystallization of the crude *meso* ligand from MeOH–diethyl ether yielded pure *meso* ligand, purification of the *rac* ligand has proven to be more problematic. Our most successful method to date involves complexation of the crude portion enriched with *rac* ligand (80% *rac*, 20% *meso*) to the tin(IV) complex $SnCl_2Et_2$[8] presumably giving a mixture of the complexes $[SnCl_2Et_2\{(R,S)$-$Ph(O)HP(CH_2)_2PH(O)Ph\}]$ **1** and $[SnCl_2Et_2\{(RR,SS)$-$Ph(O)HP(CH_2)_2PH(O)Ph\}]$ **2**. Co-ordination of the *meso* and *rac* ligands through oxygen to the Sn^{IV} centres (proposed structure of complexed *rac* ligand, complex **2**) has been established by the observation of a doublet in the

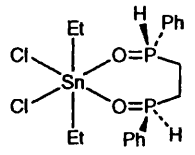

2

proton-coupled ^{31}P NMR spectrum at δ 27.8 [^{1}J(P–H) 486 Hz] corresponding to the CH_2Cl_2 soluble complex **2**. The observation of a ^{1}J(P–H) coupling constant is consistent with retention of the P–H bonds upon complexation to Sn^{IV}. Purification of the *rac* ligand is possible because [$SnCl_2Et_2$\{(*R*,*S*)-Ph(O)$HP(CH_2)_2PH$(O)Ph\}] **1** is only sparingly soluble in CH_2Cl_2 while [$SnCl_2Et_2$\{(*RR*,*SS*)-Ph(O)HP-$(CH_2)_2PH$(O)Ph\}] **2** has a much higher solubility in this solvent. After separation of complex **1** by filtration, base hydrolysis of the filtrate (ligand–Sn^{IV} decomplexation step) and repeated extraction of the aqueous layer with CH_2Cl_2 leads to the isolation of a 96% pure sample of the *rac* ligand (*RR*,*SS*)-Ph(O)$HP(CH_2)_2PH$(O)Ph **Ib**.

Synthesis and Structural Analysis of syn-[Pt\{(*R*,*S*)-Ph(O)P-$(CH_2)_2$P(OH)Ph\}$_2$] **3**.—The reaction of 2 equivalents of (*R*,*S*)-Ph(O)$HP(CH_2)_2PH$(O)Ph with [$Pt(PPh_3)_4$] proceeds with the elimination of H_2 to give the neutral Pt^{II} bis(chelate) complex *syn*-[Pt\{(*R*,*S*)-Ph(O)P$(CH_2)_2$P(OH)Ph\}$_2$] as the sole product [equation (3)]. It has been characterized by ^{31}P-\{^{1}H\} NMR

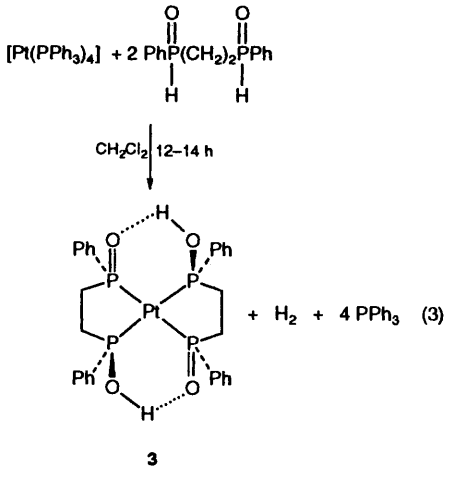

3

spectroscopy, microanalyses and by a single-crystal X-ray diffraction study. The ^{31}P-\{^{1}H\} NMR spectrum in CH_2Cl_2 consists of a singlet at δ 112.9 [$^{1}J(^{195}Pt–^{31}P)$ 2389 Hz] which originates from either a fast P–OH to P=O proton exchange that interchanges all four phosphorus atoms faster than the NMR time-scale, or is indicative of symmetrical O···H···O bridges.

The molecular structure of complex **3** is shown in Fig. 1 and selected bond lengths and angles are given in Table 1. Molecules of **3** contain a platinum atom chelated by two (*R*,*S*)-Ph(O)P$(CH_2)_2$P(OH)Ph ligands in a square-planar co-ordination geometry. Notably, the complex adopts a ligand configuration which places all four oxygen atoms in a '*syn*' relationship above the co-ordination plane. This configuration is driven by the formation of interligand hydrogen bridges (OH···O) and gives the complex a macrocyclic-type structure. Indeed this structure is reminiscent of the well known nickel dimethylglyoximate complex containing in plane interligand OH···O bridges.[9] The O···O distances of 2.468–2.516 Å are indicative of moderately strong hydrogen bonding.[10] Although the hydrogen atoms of these OH···O bridges

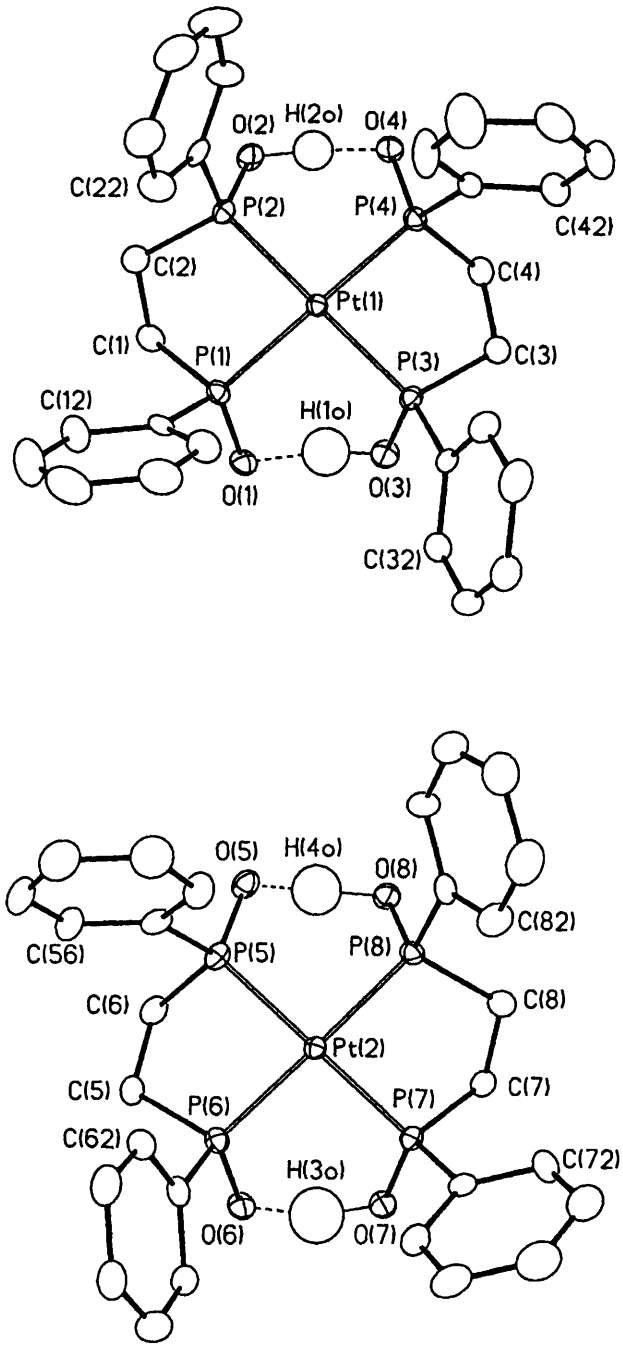

Fig. 1 Molecular structure of *syn*-[Pt\{(*R*,*S*)-Ph(O)$P(CH_2)_2$P(OH)-Ph\}$_2$] **3** showing 30% ellipsoids for all atoms in molecules 1 (top) and 2 (bottom)

are not located with a high degree of certainty, an examination of the Fourier-difference maps shows that each of the hydrogen atoms approaches a symmetrical disposition between the two oxygen atoms. A previously reported example of a complex containing a symmetrical O···H···O bridge is the Pd^{II} complex [$Pd_2(SCN)_2$\{$(Ph_2PO)_2H$\}$_2$].[11]

Spectroscopic Evidence for the Fluxional Six-co-ordinate trans-*Dihydride Intermediate syn*-[PtH_2\{(*R*,*S*)-Ph(O)P$(CH_2)_2$-P(OH)Ph\}$_2$] **4**.—Monitoring the reaction between (*R*,*S*)-Ph(O)$HP(CH_2)_2PH$(O)Ph and [$Pt(PPh_3)_4$] in CD_2Cl_2 solution by ^{31}P-\{^{1}H\} and ^{1}H NMR spectroscopy revealed the presence of a long-lived intermediate species which has been characterized *in situ* as the six co-ordinate Pt^{IV} *trans*-dihydride complex *syn*-[PtH_2\{(*R*,*S*)-Ph(O)P$(CH_2)_2$P(OH)Ph\}$_2$] **4**. Over

the course of 12–14 h this intermediate is completely converted to the thermodynamic product **3** (Scheme 4). Whilst possible short-lived species such as the Pt^{IV} *cis*-dihydride complex **5** and/or the Pt^{IV} *trans*-dihydride complex **6** are not observed spectroscopically, their existence is proposed in order to account for the rapid (< 5 min) formation of *ca.* 50% of complex **3**. The remaining 50% of **3** comes from the much slower decomposition of the *trans*-dihydride complex **4**.

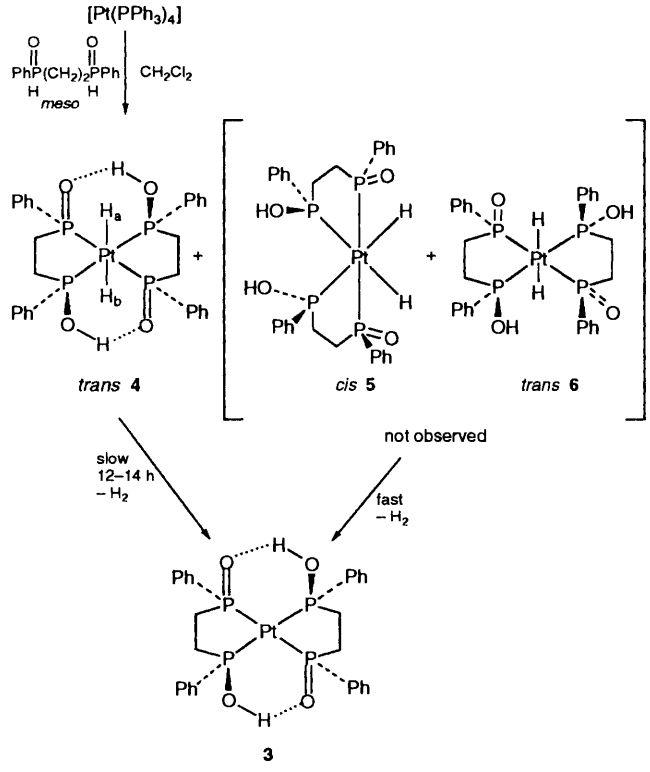

Scheme 4 Proposed reaction pathway leading to the thermodynamic product *syn*-[Pt{(*R*,*S*)-Ph(O)P(CH$_2$)$_2$P(OH)Ph}$_2$] **3**

Spectroscopic evidence for the intermediate **4** is as follows. The ^{31}P-{^1H} NMR spectrum of the reaction solution recorded 8 min after mixing consists of two approximately equal intensity singlets, one at δ 113.2 [$J(^{195}Pt$–$^{31}P)$ = 2444 Hz] corresponding to complex **3** and the other at δ 88.9 [$J(^{195}Pt$–$^{31}P)$ = 1713 Hz] being consistent with a six-co-ordinate Pt^{IV} complex containing four equivalent phosphorus atoms.[12] The ^1H NMR spectrum of the reaction solution recorded 5 min after mixing exhibits two equal intensity hydride resonances. One is a very broad unsymmetrical doublet centred at δ −7.45 [$J(^1H$–$^1H)$ *ca.* 42 and $J(^{195}Pt$–$^1H)$ 740 Hz] and the other is a fairly well resolved unsymmetrical doublet of quintets centred at δ −8.36 [$J(^1H$–$^1H)$ 45.4, $J(^{31}P$–$^1H)$ 13 and $J(^{195}Pt$–$^1H)$ 720 Hz]. The above spectral data are consistent with the six-co-ordinate Pt^{IV} complex **4** containing two inequivalent *trans* hydrides in axial positions and two chelating *meso* ligands occupying the equatorial positions in a '*syn*' configuration similar to that observed in complex **3**.

The broadness exhibited by the hydride signal at δ −7.45 suggested that one of the hydride ligands in complex **4** was undergoing a fast exchange with the P–OH protons at room temperature. The other signal at δ −8.36, a sharp doublet of quintets, clearly indicated a static hydride. In order to investigate this fluxional process, the effect on the ^1H and ^{31}P-{^1H} NMR spectra upon treating the initial reaction solution with either D_2O or HCl was studied.

Treatment of the initial reaction solution {[Pt(PPh$_3$)$_4$] + 2 *meso* ligands in CD_2Cl_2} with D_2O results in significant changes in both the ^{31}P-{^1H} and ^1H NMR spectra. The ^{31}P-{^1H} NMR spectrum recorded 8 min after mixing shows considerable reduction in the intensity of the resonance at δ 89.3 [$J(^{195}Pt$–$^{31}P)$ 1709 Hz] assigned to the Pt^{IV} *trans*-HD complex **7** compared to the intensity of the signal at δ 88.9 originating from the Pt^{IV} *trans*-dihydride **4** (observed 8 min after mixing, no D_2O added). This reduction in intensity is due to D_2O promotion of HD loss from complex **7** (see below). The signal at δ 113.4 [$J(^{195}Pt$–$^{31}P)$ 2419 Hz] probably originates from a

Table 1 Bond lengths (Å) and angles (°) for *syn*-[Pt{(*R*,*S*)-Ph(O)P(CH$_2$)$_2$P(OH)Ph}$_2$] **3**

Molecule 1				Molecule 2			
Pt(1)–P(1)	2.294(2)	P(3)–C(3)	1.828(7)	Pt(2)–P(5)	2.295(2)	P(7)–C(7)	1.835(7)
Pt(1)–P(2)	2.297(2)	P(4)–C(4)	1.830(8)	Pt(2)–P(6)	2.296(2)	P(8)–C(8)	1.838(6)
Pt(1)–P(3)	2.292(2)	P(1)–C(11)	1.811(7)	Pt(2)–P(7)	2.288(2)	P(5)–C(51)	1.810(7)
Pt(1)–P(4)	2.289(2)	P(2)–C(21)	1.806(8)	Pt(2)–P(8)	2.299(2)	P(6)–C(61)	1.817(8)
P(1)–O(1)	1.541(5)	P(3)–C(31)	1.817(7)	P(5)–O(5)	1.537(5)	P(7)–C(71)	1.800(7)
P(2)–O(2)	1.559(5)	P(4)–C(41)	1.818(8)	P(6)–O(6)	1.564(5)	P(8)–C(81)	1.810(7)
P(3)–O(3)	1.567(5)	C(1)–C(2)	1.521(9)	P(7)–O(7)	1.553(5)	C(5)–C(6)	1.532(10)
P(4)–O(4)	1.552(5)	C(3)–C(4)	1.514(9)	P(8)–O(8)	1.558(5)	C(7)–C(8)	1.532(10)
P(1)–C(1)	1.830(8)	O(1)···O(3)	2.516(10)	P(5)–C(6)	1.823(6)	O(5)···O(8)	2.484(10)
P(2)–C(2)	1.831(8)	O(2)···O(4)	2.479(10)	P(6)–C(5)	1.838(6)	O(6)···O(7)	2.468(10)
P(1)–Pt(1)–P(2)	86.3(1)	Pt(1)–P(4)–C(41)	113.1(2)	P(5)–Pt(2)–P(6)	86.0(1)	Pt(2)–P(8)–C(81)	118.5(2)
P(3)–Pt(1)–P(4)	85.7(1)	O(1)–P(1)–C(1)	109.5(3)	P(7)–Pt(2)–P(8)	86.7(1)	O(5)–P(5)–C(6)	108.9(3)
P(2)–Pt(1)–P(4)	92.0(1)	O(2)–P(2)–C(2)	110.3(3)	P(5)–Pt(2)–P(8)	92.0(1)	O(6)–P(6)–C(5)	108.7(3)
P(1)–Pt(1)–P(3)	92.9(1)	O(3)–P(3)–C(3)	108.4(3)	P(6)–Pt(2)–P(7)	92.2(1)	O(7)–P(7)–C(7)	107.8(3)
P(1)–Pt(1)–P(4)	164.5(1)	O(4)–P(4)–C(4)	107.6(3)	P(5)–Pt(2)–P(7)	162.3(1)	O(8)–P(8)–C(8)	109.6(3)
P(2)–Pt(1)–P(3)	168.5(1)	O(1)–P(1)–C(11)	109.2(3)	P(6)–Pt(2)–P(8)	170.0(1)	O(5)–P(5)–C(51)	107.9(3)
Pt(1)–P(1)–O(1)	114.2(2)	O(2)–P(2)–C(21)	107.9(3)	Pt(2)–P(5)–O(5)	114.9(2)	O(6)–P(6)–C(61)	107.0(3)
Pt(1)–P(2)–O(2)	110.8(2)	O(3)–P(3)–C(31)	106.2(3)	Pt(2)–P(6)–O(6)	113.5(2)	O(7)–P(7)–C(71)	107.8(3)
Pt(1)–P(3)–O(3)	110.7(2)	O(4)–P(4)–C(41)	109.3(3)	Pt(2)–P(7)–O(7)	113.8(2)	O(8)–P(8)–C(81)	106.0(3)
Pt(1)–P(4)–O(4)	114.6(2)	C(1)–P(1)–C(11)	105.1(3)	Pt(2)–P(8)–O(8)	110.4(2)	C(6)–P(5)–C(51)	106.9(3)
Pt(1)–P(1)–C(1)	104.1(2)	C(2)–P(2)–C(21)	106.1(3)	Pt(2)–P(5)–C(6)	102.5(2)	C(5)–P(6)–C(61)	104.8(3)
Pt(1)–P(2)–C(2)	107.9(2)	C(3)–P(3)–C(31)	103.6(3)	Pt(2)–P(6)–C(5)	107.9(2)	C(7)–P(7)–C(71)	108.0(3)
Pt(1)–P(3)–C(3)	108.0(2)	C(4)–P(4)–C(41)	107.6(4)	Pt(2)–P(7)–C(7)	104.5(2)	C(8)–P(8)–C(81)	103.9(4)
Pt(1)–P(4)–C(4)	104.2(2)	P(1)–C(1)–C(2)	111.5(6)	Pt(2)–P(8)–C(8)	108.1(2)	P(5)–C(6)–C(5)	112.3(5)
Pt(1)–P(1)–C(11)	114.2(2)	P(2)–C(2)–C(1)	112.4(6)	Pt(2)–P(5)–C(51)	115.2(2)	P(6)–C(5)–C(6)	111.6(4)
Pt(1)–P(2)–C(21)	113.7(2)	P(3)–C(3)–C(4)	112.8(5)	Pt(2)–P(6)–C(61)	114.6(2)	P(7)–C(7)–C(8)	112.0(4)
Pt(1)–P(3)–C(31)	119.3(2)	P(4)–C(4)–C(3)	110.7(5)	Pt(2)–P(7)–C(71)	114.6(2)	P(8)–C(8)–C(7)	112.0(4)

mixture of the fully deuteriated complexes **8** (major) and **3** (minor) [equation (4)].

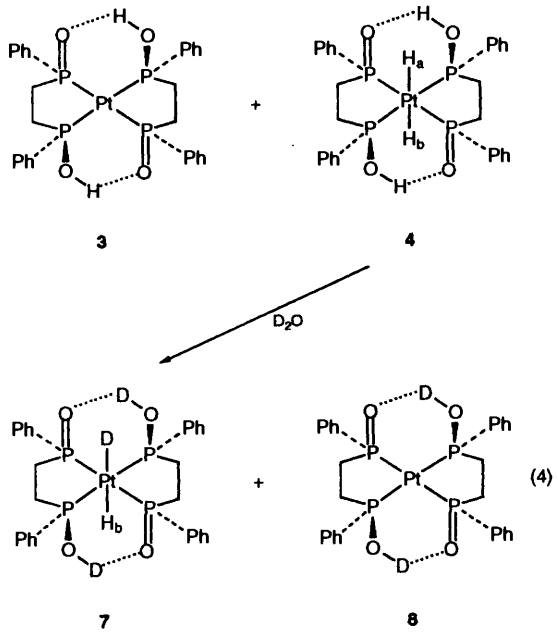

The ^1H NMR spectrum exhibits a new broad resonance at δ −8.25 [$J(^{195}Pt-^1H)$ *ca.* 730 Hz]. Notably this signal does not exhibit a *trans*-($^1H-^1H$) coupling constant and likely originates from the Pt^{IV} *trans*-HD complex **7** in equation (4). Lower intensity resonances are observed at δ −7.65 and −8.4. These signals are assigned to the *trans*-dihydride complex **4**.

In a separate experiment, HCl gas was bubbled through the reaction solution for 2 min and the $^{31}P-\{^1H\}$ and ^1H NMR spectra recorded. The $^{31}P-\{^1H\}$ NMR spectrum showed singlet resonances originating from the dicationic complex *anti*-[Pt{(*R*,*S*)-Ph(OH)P$(CH_2)_2$P(OH)Ph}$_2$]Cl_2 **9** (15% yield) [δ 118.4, $J(^{195}Pt-^{31}P)$ 2589 Hz], the tentatively proposed dicationic complex *syn*-[Pt{(*R*,*S*)-Ph(OH)P$(CH_2)_2$P(OH)Ph}$_2$]-Cl_2 **10** (55% yield) [δ 120.7, $J(^{195}Pt-^{31}P)$ 2486 Hz] (structural characteristics of **10** are discussed later) and the dicationic Pt^{IV} *trans*-dihydride complex *syn*-[PtH_2\{(*R*,*S*)-Ph(OH)P$(CH_2)_2$-P(OH)Ph}$_2$]Cl_2 **11** (30% yield) [δ 100.6, $J(^{195}Pt-^{31}P)$ 1688 Hz] [equation (5)]. The ^1H NMR spectrum exhibits two equal intensity doublet of quintet hydride resonances, one at δ −7.2 [$J(^1H-^1H)$ 47.3, $J(^{31}P-^1H)$ 10 and $J(^{195}Pt-^1H)$ 702 Hz] and the other at δ −7.85 [$J(^1H-^1H)$ 47.6, $J(^{31}P-^1H)$ 13.7 and $J(^{195}Pt-^1H)$ 690 Hz]. These hydride signals are assigned to the *trans*-hydride ligands H_a and H_b respectively in complex **11**. After 11 h the $^{31}P-\{^1H\}$ NMR spectrum shows that only a trace of the complex remains.

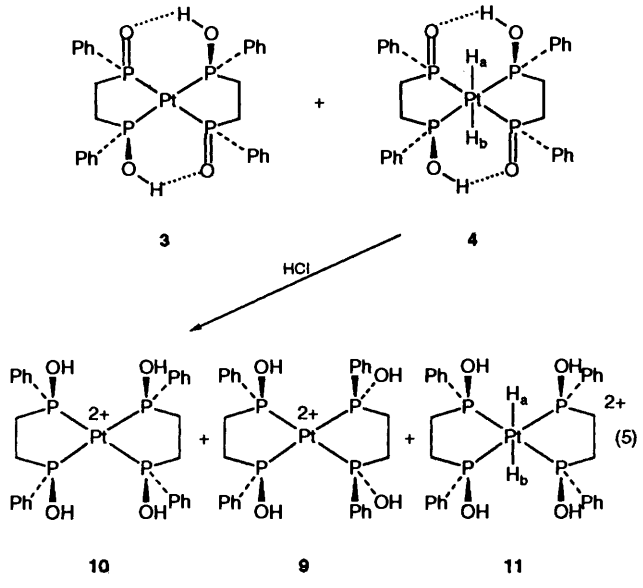

The above $^{31}P-\{^1H\}$ and ^1H NMR data support the structural assignment of the reaction intermediate in Scheme 4 as the Pt^{IV} *trans*-dihydride complex *syn*-[PtH_2\{(*R*,*S*)-Ph(O)P-$(CH_2)_2$P(OH)Ph}$_2$] **4**. The data also suggest that the hydride *trans* disposed to the oxygens (H_b) is static and that *cis* to the oxygens (H_a) undergoes a rapid proton exchange with the P–OH protons. This is supported by the observations that the hydride signal at δ −7.45, assigned to H_a, dramatically drops in intensity upon addition of D_2O, and resolves to a doublet of quintets upon addition of dry HCl. Presumably, the HCl protonates both of the phosphoryl oxygens (P=O) thereby slowing down, if not arresting completely, the mechanism by which H_a is exchanged with the OH protons. This observation excludes a mechanism involving initial protonation of the H_a hydride to give a Pt^{IV} η^2-H_2 complex which then transfers H_a to an acceptor phosphoryl oxygen (P=O) to regenerate complex **4**. Scheme 5 outlines a possible mechanism by which the H_a hydride of complex **4** undergoes a rapid proton exchange with the P–OH protons. Initial proton transfer of H_a from Pt to a phosphoryl oxygen gives a Pt^{II} five-co-ordinate monohydride, which is then reprotonated by a P–OH group to regenerate the dihydride complex **4**. Proton transfer from Pt to a P=O group is reasonable in view of the fact that a Pt^{IV} hydride would be expected to be sufficiently acidic in nature;[13] and secondly, the observation that the fluxional process is arrested by HCl addition is consistent with the requirement that an accessible P=O group be present to accept H_a from the Pt centre.

Relative Rate Studies into the Decomposition of the Intermediate Platinum(IV) trans-*Dihydride Complex* **4**.—In each of three separate experiments [$Pt(PPh_3)_4$] and (*R*,*S*)-Ph(O)HP-$(CH_2)_2$PH(O)Ph (1:2 molar ratio) were dissolved in CD_2Cl_2. The resultant solutions were then subjected to different conditions [part 1: no change 'blank run', 0.8 cm^3 CD_2Cl_2; part 2: two drops of D_2O added, 0.8 cm^3 CD_2Cl_2; part 3: HCl(g) added for 2 min, 1.0 cm^3 CD_2Cl_2] and the progress of each reaction monitored by $^{31}P-\{^1H\}$ NMR spectroscopy. Monitoring the reaction in part 2 (D_2O added) showed that complete conversion of the Pt^{IV} *trans*-HD complex **7** to the deuteriated Pt^{II} bis(chelate) complex **8** occurred after only 1.5 h. This represents approximately a nine-fold increase in the rate of H_2/HD loss from the initially formed Pt^{IV} *trans*-dihydride/HD

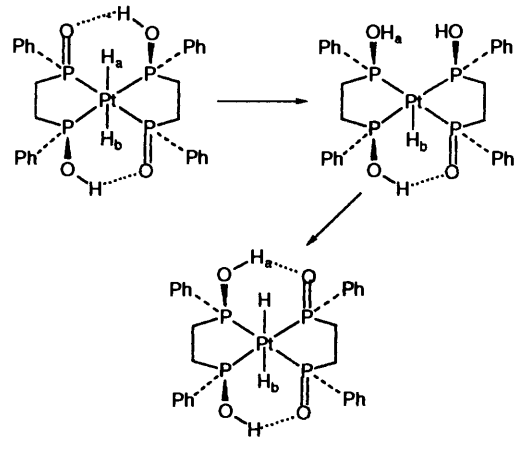

Scheme 5 Mechanistic proposal for the observed proton exchange between the H_a hydride and the P–OH protons in *syn*-[PtH_2\{(*R*,*S*)-Ph(O)P$(CH_2)_2$P(OH)Ph}$_2$] **4**

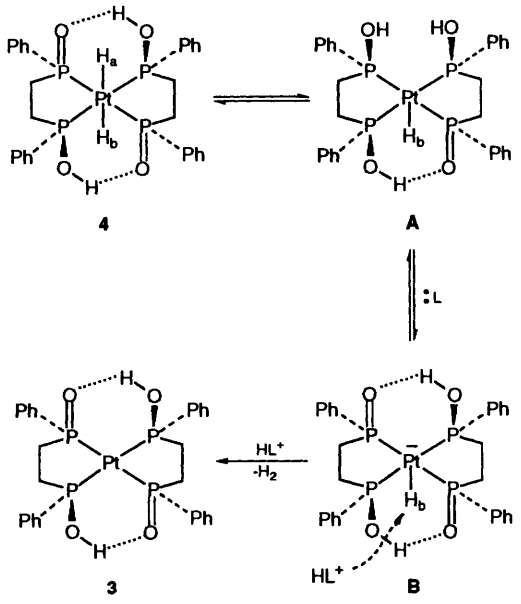

Scheme 6 Proposed mechanism for the decomposition of the Pt^{IV} *trans*-dihydride **4** to the thermodynamic complex **3**

complex compared to conditions in which no D_2O has been added (part 1 'blank run', reaction time 12–14 h). In contrast, the addition of HCl to the reaction solution in part 3 results in the formation of the dicationic Pt^{IV} *trans*-dihydride complex **11** which slowly converts over the course of 12 h to a mixture of the dicationic complexes *syn*-[Pt{(*R*,*S*)-Ph(OH)P(CH_2)$_2$P(OH)Ph}$_2$]Cl_2 **10** and *anti*-[Pt{(*R*,*S*)-Ph(OH)P(CH_2)$_2$P(OH)Ph}$_2$]Cl_2 **9**. A proposed mechanism accounting for the observed differences in the rate of decomposition of the initially formed Pt^{IV} dihydride complex **4** to complex **3** or its deuterium analogue **8** in parts 1 and 2 is shown in Scheme 6. Here it is proposed that initial proton transfer from Pt^{IV} to a P=O group gives a square-pyramidal Pt^{II} complex **A**. Intermolecular proton transfer from this complex to a base L: (either D_2O or oxygen centres on complexes **3** or **4**) gives an anionic square pyramidal Pt^{II} hydride **B** and HL^+. Protonation of complex **B** by HL^+ leads to the extrusion of H_2 and formation of the thermodynamic product **3**. Such a mechanism indicates that the stability of the Pt^{IV} *trans*-dihydride **4** is dependent on protecting H_b from H^+ sources. In **4**, H_b is protected by four phenyl groups. The mechanism also explains why Pt^{IV} dihydride intermediates such as **5** and **6** (Scheme 4) rapidly lose H_2 to give **3** since both hydrides in these intermediates are adjacent to OH proton sources. The suggested mechanism is consistent with recent studies in which hydrogen bonds from *cis*-ligand sites to a metal–hydrido ligand have been observed.[14]

Reaction of Complex **3** *with Dry* HCl: *Preparation and Structural Analysis of syn*-[Pt{(*R*,*S*)-Ph(O)P(CH_2)$_2$P(OH)Ph}{(*R*,*S*)-Ph(OH)P(CH_2)$_2$P(OH)Ph}]Cl **12**.—By briefly treating a CH_2Cl_2 solution of complex **3** with dry HCl the monocationic complex **12** was rapidly produced and isolated in high yield [equation (6)]. Interestingly enough, under these conditions complex **12** does not readily undergo further protonation by HCl. The complex was characterized by ^{31}P-{^1H} NMR spectroscopy and its structure determined by a single-crystal X-ray diffraction study. Its ^{31}P-{^1H} NMR spectrum in CH_2Cl_2 consists of a broad resonance at δ 119.2 [J(^{195}Pt–^{31}P) 2465 Hz]. The broadness of this signal is indicative of a fast OH proton exchange mechanism which at room temperature effectively interchanges all four phosphorus atoms faster than the NMR time-scale. Under more acidic conditions (prolonged exposure to HCl in CH_2Cl_2)

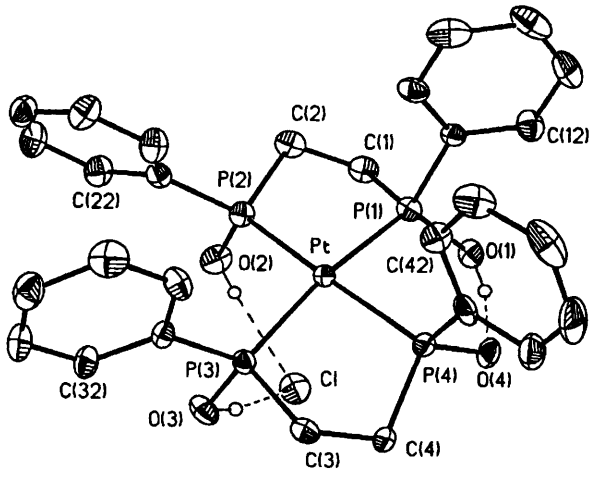

Fig. 2 Molecular structure of *syn*-[Pt{(*R*,*S*)-Ph(O)P(CH_2)$_2$P(OH)Ph}{(*R*,*S*)-Ph(OH)P(CH_2)$_2$P(OH)Ph}]Cl **12**

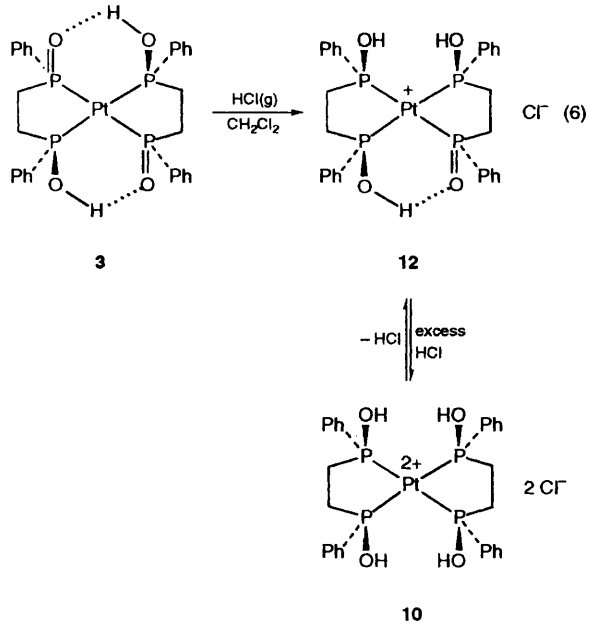

the broad resonance at δ 119.2 shifts to 120.7 [J(^{195}Pt–^{31}P) 2486 Hz] and sharpens considerably. This observation suggests that in the presence of excess HCl the monocationic complex **12** is protonated to give the dicationic complex *syn*-[Pt{(*R*,*S*)-Ph(OH)P(CH_2)$_2$P(OH)Ph}$_2$]Cl_2 **10** [equation (6)] in which the '*syn*' oxygen configuration has been retained. We have been unable to isolate complex **10** for the purpose of an X-ray diffraction study. An alternative explanation assigns the broadness of the signals of **12** to proton exchange with a small amount of **3**. The concentration of **3** is suppressed by the addition of excess HCl.

The structure of complex **12** is shown in Fig. 2 and selected bond lengths and angles are given in Table 2. A noteworthy feature is that molecules of **12** have retained the '*syn*' oxygen configuration that was observed in the structure of complex **3** (Fig. 1). Moreover, whilst one interligand hydrogen bridge (O–H···O) has remained intact, protonation has led to hydrogen-bonding interactions between Cl^- and the two OH groups [Cl···O distances 2.972(5)–2.980(5) Å]. Typical Cl^-···H–O bonds exhibit Cl···O distances of < 3.2 Å.[15] The above results show that both the neutral and monocationic Pt^{II} bis(chelate) complexes *syn*-[Pt{(*R*,*S*)-Ph(O)P(CH_2)$_2$P(OH)Ph}$_2$] **3** and *syn*-[Pt{(*R*,*S*)-Ph(O)P(CH_2)$_2$-

Table 2 Bond lengths (Å) and angles (°) for *syn*-[Pt{(*R*,*S*)-Ph(O)P(CH$_2$)$_2$P(OH)Ph}{(*R*,*S*)-Ph(OH)P(CH$_2$)$_2$P(OH)Ph}]Cl **12**

Pt–P(1)	2.288(2)	P(3)–C(31)	1.807(8)
Pt–P(2)	2.302(2)	P(4)–C(41)	1.809(10)
Pt–P(3)	2.305(2)	C(1)–C(2)	1.539(13)
Pt–P(4)	2.294(2)	C(3)–C(4)	1.526(12)
P(1)–O(1)	1.557(7)	O(1)–H(1a)	0.91(11)
P(2)–O(2)	1.593(8)	O(2)–H(2a)	0.75(8)
P(3)–O(3)	1.595(7)	O(3)–H(3a)	0.92(10)
P(4)–O(4)	1.534(6)	O(4) · · · H(1a)	1.58(10)
P(1)–C(1)	1.803(9)	O(1) · · · O(4)	2.473(10)
P(2)–C(2)	1.823(9)	O(2) · · · Cl	2.980(5)
P(3)–C(3)	1.815(9)	O(3) · · · Cl	2.972(5)
P(4)–C(4)	1.820(10)	Cl · · · H(3a)	2.06(10)
P(1)–C(11)	1.811(8)	Cl · · · H(2a)	2.24(10)
P(2)–C(21)	1.791(9)		
P(1)–Pt–P(2)	85.3(1)	O(3)–P(3)–C(3)	105.6(4)
P(3)–Pt–P(4)	85.3(1)	O(4)–P(4)–C(4)	109.5(4)
P(2)–Pt–P(3)	100.5(1)	O(1)–P(1)–C(11)	106.4(4)
P(1)–Pt–P(4)	88.0(1)	O(2)–P(2)–C(21)	103.5(4)
P(1)–Pt–P(3)	171.5(1)	O(3)–P(3)–C(31)	103.8(4)
P(2)–Pt–P(4)	169.6(1)	O(4)–P(4)–C(41)	108.7(4)
Pt–P(1)–O(1)	114.4(1)	C(1)–P(1)–C(11)	107.1(4)
Pt–P(2)–O(2)	113.0(1)	C(2)–P(2)–C(21)	107.4(4)
Pt–P(3)–O(3)	112.6(3)	C(3)–P(3)–C(31)	104.5(4)
Pt–P(4)–O(4)	114.7(3)	C(4)–P(4)–C(41)	104.7(4)
Pt–P(1)–C(1)	108.0(3)	P(1)–C(1)–C(2)	109.8(6)
Pt–P(2)–C(2)	107.2(3)	P(2)–C(2)–C(1)	109.7(6)
Pt–P(3)–C(3)	107.4(3)	P(3)–C(3)–C(4)	110.3(6)
Pt–P(4)–C(4)	105.9(3)	P(4)–C(4)–C(3)	108.5(6)
Pt–P(1)–C(11)	113.3(3)	P(1)–O(1)–H(1a)	111(7)
Pt–P(2)–C(21)	120.9(3)	P(2)–O(2)–H(2a)	116(6)
Pt–P(3)–C(31)	121.7(3)	P(3)–O(3)–H(3a)	106(6)
Pt–P(4)–C(41)	112.9(3)	O(1)–H(1a) · · · O(4)	163(7)
O(1)–P(1)–C(1)	107.3(4)	O(2) · · · Cl · · · O(3)	77.7(2)
O(2)–P(2)–C(2)	103.4(4)	H(2a) · · · Cl · · · H(3a)	83(10)

P(OH)Ph}{(*R*,*S*)-Ph(OH)P(CH$_2$)$_2$P(OH)Ph}]Cl **12** adopt '*syn*' oxygen configurations driven by the formation of intramolecular interligand O–H · · · O bridges. In the next section the structural consequences of eliminating the opportunity for O–H · · · O hydrogen bonding by formal diprotonation of *syn*-[Pt{(*R*,*S*)-Ph(O)P(CH$_2$)$_2$P(OH)Ph}$_2$] **3** are presented.

Preparation and Structural Analysis of anti-[Pt{(*R*,*S*)-Ph(OH)P(CH$_2$)$_2$P(OH)Ph}$_2$]Cl$_2$ **9**.—The reaction of Zeise's dimer with 2 equivalents per Pt of (*R*,*S*)-Ph(O)HP(CH$_2$)$_2$-PH(O)Ph leads to the isolation of the dicationic complex **9** [equation (7)] in low yield. The ^{31}P-{^{1}H} NMR spectrum of **9**

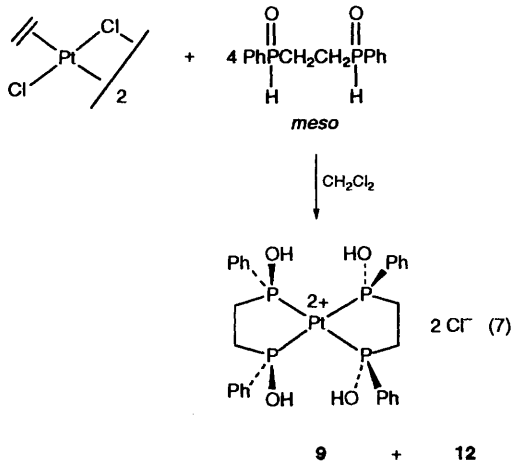

Table 3 Bond lengths (Å) and angles (°) for *anti*-[Pt{(*R*,*S*)-Ph(OH)P(CH$_2$)$_2$P(OH)Ph}$_2$]Cl$_2$ **9**

Pt–P(1)	2.291(1)	P(2)–C(21)	1.793(5)
Pt–P(2)	2.299(1)	C(1)–C(2)	1.503(6)
P(1)–O(1)	1.578(3)	Cl · · · O(2)	2.975(1)
P(2)–O(2)	1.588(3)	Cl · · · O(1)	2.972(1)
P(1)–C(1)	1.812(5)	H(1) · · · Cl	2.01
P(2)–C(2)	1.827(5)	H(2) · · · Cl	2.02
P(1)–C(11)	1.797(4)		
P(1)–Pt–P(2)	84.3(1)	O(1)–P(1)–C(1)	106.5(2)
P(2)–Pt–P(1a)	95.7(1)	O(2)–P(2)–C(2)	106.1(2)
P(1)–Pt–P(1a)	180.0	O(1)–P(1)–C(11)	104.1(2)
Pt–P(1)–O(1)	111.9(1)	O(2)–P(2)–C(21)	103.4(2)
Pt–P(2)–O(2)	115.1(1)	C(1)–P(1)–C(11)	104.4(2)
Pt–P(1)–C(1)	104.7(2)	C(2)–P(2)–C(21)	107.3(2)
Pt–P(2)–C(2)	108.0(2)	P(1)–C(1)–C(2)	109.7(3)
Pt–P(1)–C(11)	123.9(1)	P(2)–C(2)–C(1)	112.8(3)
Pt–P(2)–C(21)	116.3(1)	O(1) · · · Cl · · · O(2)	89.0(1)

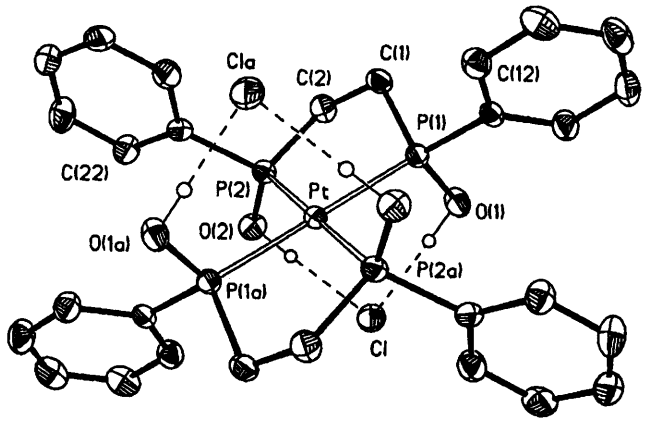

Fig. 3 Molecular structure of *anti*-[Pt{(*R*,*S*)-Ph(OH)P(CH$_2$)$_2$P-(OH)Ph}$_2$]Cl$_2$ **9**

in CH_2Cl_2 shows a sharp singlet resonance at δ 117.5 [J(^{195}Pt–^{31}P) 2587 Hz] consistent with four equivalent phosphorus-donor atoms.

The molecular structure of **9** as determined by single-crystal X-ray diffraction is shown in Fig. 3. The asymmetric unit consists of one half of one dication and one chloride anion. Selected bond lengths and angles are given in Table 3. In contrast to both the neutral complex **3** and the monocationic complex **12** which adopt *syn* ligand configurations about the platinum atom, molecules of **9** adopt an *anti* ligand configuration. Presumably this structure minimizes Cl^- · · · Cl^- electrostatic repulsion while at the same time allows each Cl^- ion to hydrogen bond with two P–OH groups [Cl · · · O distances 2.972(1)–2.975(1) Å]. The Pt · · · Cl^- distances of 3.399(2) Å represent non-bonding interactions.

Reaction of Complex **3** *with* BF_3·Et_2O: *Stereoselective Synthesis and Structure Analysis of syn*-[Pt{[(*R*,*S*)-Ph(O)P-(CH$_2$)$_2$P(O)Ph]BF$_2$}$_2$]·CH_2Cl_2 **13**.—Previous studies have shown that complexes containing the fragment 'M(OPPh$_2$)-(PPh$_2$OH)' readily react with electrophilic reagents such as BF_3·Et_2O and $SiCl_2Me_2$ to give complexes containing the fragment 'M(PPh$_2$O–E–OPPh$_2$)' (E = BF_2 or $SiMe_2$).[16,17] Thus addition of an excess of BF_3·Et_2O to a CH_2Cl_2 solution of complex **3** affords the macrocyclic complex *syn*-[Pt{[(*R*,*S*)-Ph(O)P(CH$_2$)$_2$P(O)Ph]BF$_2$}$_2$]·CH_2Cl_2 **13** [equation (8)]. The ^{31}P-{^{1}H} NMR spectrum of **13** exhibits a singlet resonance at δ 119.5 [J(^{195}Pt–^{31}P) 2459 Hz] consistent with four equivalent phosphorus atoms. Two broad doublet resonances are observed in the ^{19}F NMR spectrum, one at δ −134.8

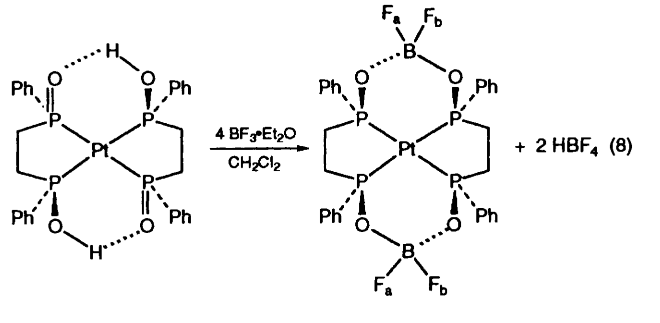

3 13

$[J(^{19}F-^{19}F)$ 59] and the other at δ −139.1 $[J(^{19}F-^{19}F)$ 60 Hz]. These signals are assigned to the inequivalent fluorine nuclei F_a and F_b.

The structure of complex **13** determined by single-crystal X-ray diffraction is shown in Fig. 4. There is one dichloromethane solvent molecule present in the formula which is also the asymmetric unit. Selected bond lengths and angles are given in Table 4. Molecules of **13** contain a platinum atom bonded to the macrocyclic ligand $\{[(R,S)\text{-Ph(O)P(CH}_2)_2\text{P(O)Ph]BF}_2\}_2$ in a square-planar co-ordination geometry. In contrast to its solution behaviour wherein there are two sets of chemically non-equivalent fluorine atoms, the solid-state structure of **13** exhibits four non-equivalent fluorine atoms. Whilst F(3) and F(4) occupy axial and equatorial type positions respectively in a 'chair-like' six-membered ring (Pt–P–O–B–O–P), F(2) and F(1) occupy axial and equatorial type positions respectively in a 'boat-like' six-membered ring (Pt–P–O–B–O–P).

The reaction of complex **3** with $BF_3 \cdot Et_2O$ to give **13** represents a rare stereoselective synthesis of a phosphorus-based macrocyclic complex. The selectivity originates from both the template effect and the '*syn*' ligand arrangement driven by the formation of interligand O–H···O hydrogen bridges in complex **3**. A previous example of a stereoselective synthesis of a phosphorus-based macrocyclic complex is the Pd^{II} complex **14** prepared by a simple one-pot reaction of $[Pd(acac)_2]$ (acac = acetylacetonate) with $HMeP(CH_2)_2PMeH$ and HCl [equation (9)].[18]

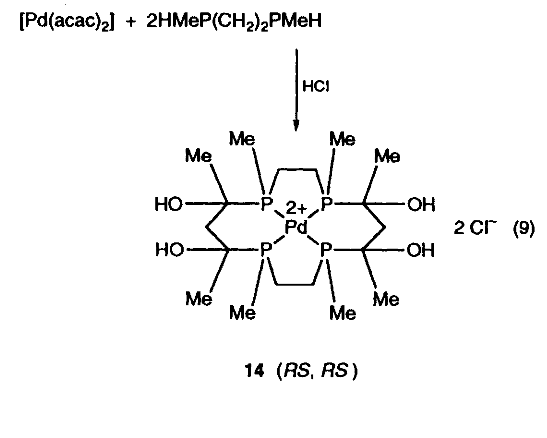

14 (*RS*, *RS*)

Preparation and Structural Characterization of Complexes containing the Racemic Ligand **Ib**.—Treatment of a CH_2Cl_2 solution containing $[Pt(PPh_3)_4]$ with 2 equivalents of (*RR*,*SS*)-$Ph(O)HP(CH_2)_2PH(O)Ph$ resulted in the precipitation of a white CH_2Cl_2 insoluble solid consisting of a mixture of *meso*-$[\{Pt[(R,R)\text{-Ph(O)P(CH}_2)_2\text{P(OH)Ph}][(S,S)\text{-Ph(O)P(CH}_2)_2\text{P(OH)Ph}]\}_n]$ **15** and presumably *rac*-$[\{Pt[(RR,RR)\text{-Ph(O)P(CH}_2)_2\text{P(OH)Ph}]_2\}_n]$ and its (*SS*,*SS*) analogue **16** [equation (10)]. While the *meso* diastereomer **15** has been structurally characterized by a single-crystal X-ray diffraction study (Fig. 5), only indirect evidence for the *rac* diastereomer **16** has been obtained thus far. This evidence comes from the structural characterization of two isomeric derivatives formed when a suspension of the CH_2Cl_2 insoluble white solid (**15** + **16**) in CH_2Cl_2 was treated with dry HCl [equation (11)]. The ^{31}P-

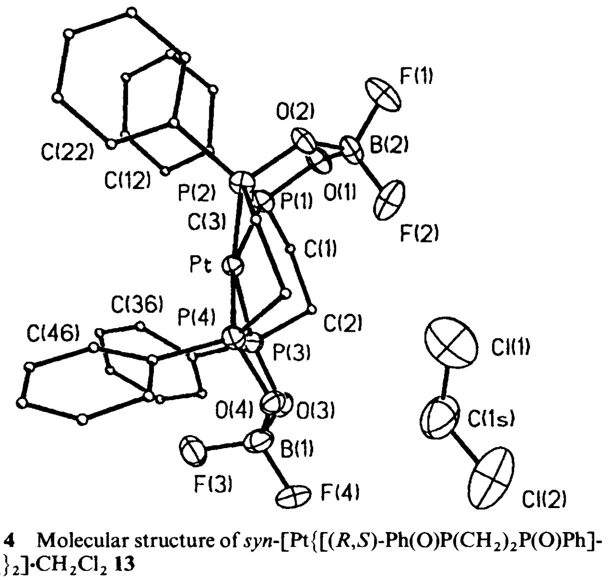

Fig. 4 Molecular structure of *syn*-$[Pt\{[(R,S)\text{-Ph(O)P(CH}_2)_2\text{P(O)Ph]BF}_2\}_2]\cdot CH_2Cl_2$ **13**

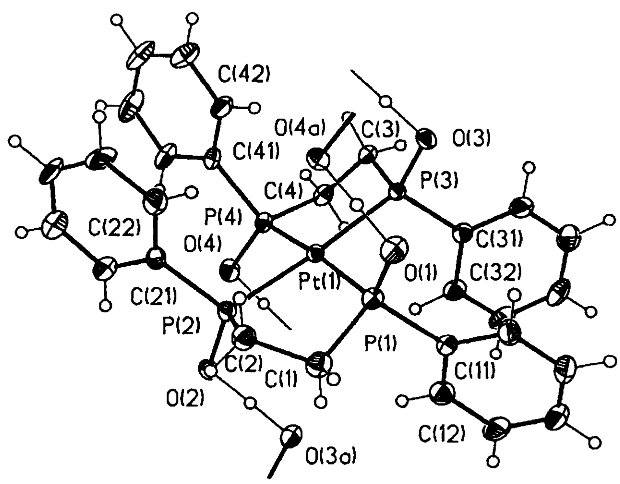

Fig. 5 Molecular structure of *meso*-$[\{Pt[(R,R)\text{-Ph(O)P(CH}_2)_2\text{P(OH)Ph}][(S,S)\text{-Ph(O)P(CH}_2)_2\text{P(OH)Ph}]\}_n]$ **15**

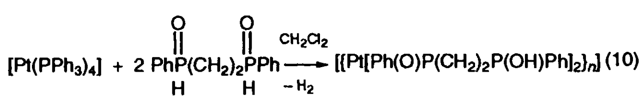

rac 15, 16

(*RR*, *SS*) or {(*RR*, *RR*)/(*SS*, *SS*)}

(*RR*, *SS*)- or {(*RR*, *RR*)/(*SS*, *SS*)}-$[\{Pt[Ph(O)P(CH_2)_2P(OH)Ph]_2\}_n]$

15, 16

CH_2Cl_2 | HCl

(*RR*, *SS*)- or {(*RR*, *RR*)/(*SS*, *SS*)}-$[Pt\{Ph(OH)P(CH_2)_2P(OH)Ph\}_2]Cl_2$ (11)

17, 18

Table 4 Bond lengths (Å) and angles (°) for *syn*-[Pt{[(*R*,*S*)-Ph(O)P(CH$_2$)$_2$P(O)Ph]BF$_2$}$_2$]·CH$_2$Cl$_2$ **13**

Pt–P(1)	2.293(3)	P(3)–C(31)	1.796(12)
Pt–P(2)	2.296(3)	P(4)–C(41)	1.803(11)
Pt–P(3)	2.281(3)	C(1)–C(2)	1.530(16)
Pt–P(4)	2.279(3)	C(3)–C(4)	1.539(16)
P(1)–O(1)	1.564(8)	O(1)–B(2)	1.498(16)
P(2)–O(2)	1.560(8)	O(2)–B(2)	1.477(16)
P(3)–O(4)	1.573(8)	O(3)–B(1)	1.472(18)
P(4)–O(3)	1.567(8)	O(4)–B(1)	1.530(18)
P(1)–C(1)	1.852(11)	F(1)–B(2)	1.350(17)
P(2)–C(3)	1.838(11)	F(2)–B(2)	1.340(18)
P(3)–C(2)	1.832(11)	F(3)–B(1)	1.386(18)
P(4)–C(4)	1.819(12)	F(4)–B(1)	1.357(18)
P(1)–C(11)	1.810(12)	Cl(1)–C(1s)	1.610(24)
P(2)–C(21)	1.828(13)	Cl(2)–C(1s)	1.340(18)
P(1)–Pt–P(2)	90.6(1)	C(1)–P(1)–C(11)	106.8(5)
P(3)–Pt–P(4)	93.2(1)	C(2)–P(3)–C(31)	104.5(5)
P(1)–Pt–P(3)	85.6(1)	C(3)–P(2)–C(21)	106.4(5)
P(2)–Pt–P(4)	86.1(1)	C(4)–P(4)–C(41)	107.6(5)
P(2)–Pt–P(3)	164.6(1)	P(1)–C(1)–C(2)	110.9(7)
P(1)–Pt–P(4)	162.7(1)	P(2)–C(3)–C(4)	110.4(7)
Pt–P(1)–O(1)	109.6(3)	P(3)–C(2)–C(1)	107.8(8)
Pt–P(2)–O(2)	110.5(3)	P(4)–C(4)–C(3)	109.1(8)
Pt–P(3)–O(4)	116.2(3)	P(1)–O(1)–B(2)	131.1(8)
Pt–P(4)–O(3)	114.2(3)	P(2)–O(2)–B(2)	130.6(8)
Pt–P(1)–C(1)	107.3(4)	P(4)–O(3)–B(1)	123.1(8)
Pt–P(2)–C(3)	107.1(4)	P(3)–O(4)–B(1)	123.0(8)
Pt–P(3)–C(2)	104.1(4)	O(3)–B(1)–O(4)	110.1(11)
Pt–P(4)–C(4)	103.0(4)	O(1)–B(2)–O(2)	111.6(10)
Pt–P(1)–C(11)	119.5(4)	F(1)–B(2)–F(2)	115.0(11)
Pt–P(2)–C(21)	120.0(4)	F(3)–B(1)–F(4)	112.9(12)
Pt–P(3)–C(31)	115.7(4)	F(3)–B(1)–O(4)	107.2(11)
Pt–P(4)–C(41)	118.3(4)	F(3)–B(1)–O(3)	111.5(12)
O(1)–P(1)–C(1)	107.5(5)	F(4)–B(1)–O(4)	104.8(11)
O(2)–P(2)–C(3)	107.9(5)	F(4)–B(1)–O(3)	110.0(12)
O(3)–P(4)–C(4)	104.8(5)	F(1)–B(2)–O(2)	106.6(11)
O(4)–P(3)–C(2)	104.5(5)	F(1)–B(2)–O(1)	105.2(10)
O(1)–P(1)–C(11)	105.6(5)	F(2)–B(2)–O(1)	108.2(11)
O(2)–P(2)–C(21)	104.5(5)	F(2)–B(2)–O(2)	110.1(11)
O(3)–P(4)–C(41)	107.8(4)	Cl(1)–C(1s)–Cl(2)	110.1(11)
O(4)–P(3)–C(31)	110.2(5)		

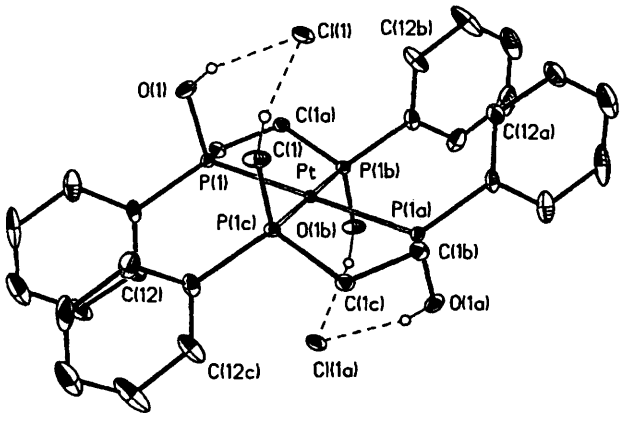

Fig. 6 Molecular structure of *meso*-[Pt{(*R*,*R*)-Ph(OH)P(CH$_2$)$_2$P(OH)Ph}{(*S*,*S*)-Ph(OH)P(CH$_2$)$_2$P(OH)Ph}]Cl$_2$ **17**

{^{1}H} NMR spectrum recorded of the resultant solution showed two singlets; one at δ 116.8 [J(^{195}Pt–^{31}P) 2629 Hz] and the other at δ 117.7 [J(^{195}Pt–^{31}P) 2525 Hz] in a relative intensity of *ca.* 1:2. Addition of diethyl ether to this solution gave two morphologically different colourless crystals which have been structurally characterized as the dicationic complexes *meso*-[Pt{(*R*,*R*)-Ph(OH)P(CH$_2$)$_2$P(OH)Ph}{(*S*,*S*)-Ph(OH)P(CH$_2$)$_2$P(OH)Ph}]Cl$_2$ **17** and *rac*-[Pt{(*RR*,*RR*)- or (*SS*,*SS*)-Ph(OH)P(CH$_2$)$_2$P(OH)Ph}$_2$]Cl$_2$ **18** by X-ray diffraction studies. The formation of **18** lends support to the proposal that the original CH$_2$Cl$_2$ insoluble white solid contains *rac*-

Table 5 Bond lengths (Å) and angles (°) for *meso*-[{Pt[(*R*,*R*)-Ph(O)P(CH$_2$)$_2$P(OH)Ph][(*S*,*S*)-Ph(O)P(CH$_2$)$_2$P(OH)Ph]}$_n$] **15**

Pt(1)–P(1)	2.311(2)	P(3)–C(3)	1.828(6)
Pt(1)–P(2)	2.294(2)	P(4)–C(4)	1.833(6)
Pt(1)–P(3)	2.304(2)	P(1)–C(11)	1.813(7)
Pt(1)–P(4)	2.308(2)	P(2)–C(21)	1.800(7)
P(1)–O(1)	1.539(5)	P(3)–C(31)	1.802(7)
P(2)–O(2)	1.544(5)	P(4)–C(41)	1.814(6)
P(3)–O(3)	1.551(5)	C(1)–C(2)	1.560(10)
P(4)–O(4)	1.550(5)	C(3)–C(4)	1.538(11)
P(1)–C(1)	1.812(7)	O(1)···O(4a)	2.421(10)
P(2)–C(2)	1.832(7)	O(2)···O(3a)	2.440(10)
P(1)–Pt(1)–P(3)	95.6(1)	O(1)–P(1)–C(1)	108.1(3)
P(1)–Pt(1)–P(2)	85.3(1)	O(2)–P(2)–C(2)	108.3(3)
P(2)–Pt(1)–P(4)	92.9(1)	O(3)–P(3)–C(3)	107.0(3)
P(3)–Pt(1)–P(4)	86.6(1)	O(4)–P(4)–C(4)	107.2(3)
P(1)–Pt(1)–P(4)	174.2(1)	O(1)–P(1)–C(11)	105.9(3)
P(3)–Pt(1)–P(2)	175.5(1)	O(2)–P(2)–C(21)	108.1(3)
Pt(1)–P(1)–O(1)	117.1(2)	O(3)–P(3)–C(31)	105.5(3)
Pt(1)–P(2)–O(2)	118.0(2)	O(4)–P(4)–C(41)	105.1(3)
Pt(1)–P(3)–O(3)	118.1(2)	C(1)–P(1)–C(11)	100.5(3)
Pt(1)–P(4)–O(4)	118.0(2)	C(2)–P(2)–C(21)	105.2(3)
Pt(1)–P(1)–C(1)	106.4(3)	C(3)–P(3)–C(31)	102.6(3)
Pt(1)–P(2)–C(2)	106.1(3)	C(4)–P(4)–C(41)	102.0(3)
Pt(1)–P(3)–C(3)	107.3(2)	P(1)–C(1)–C(2)	107.7(4)
Pt(1)–P(4)–C(4)	104.6(2)	P(2)–C(2)–C(1)	106.4(4)
Pt(1)–P(1)–C(11)	117.3(2)	P(3)–C(3)–C(4)	110.0(4)
Pt(1)–P(2)–C(21)	110.4(2)	P(4)–C(4)–C(3)	110.4(4)
Pt(1)–P(3)–C(31)	115.0(2)	P(1)–O(1)···O(4a)	124.7(9)
Pt(1)–P(4)–C(41)	118.3(2)	P(2)–O(2)···O(3a)	119.4(9)

Table 6 Bond lengths (Å) and angles (°) for *meso*-[Pt{(*R*,*R*)-Ph(OH)P(CH$_2$)$_2$P(OH)Ph}{(*S*,*S*)-Ph(OH)P(CH$_2$)$_2$P(OH)Ph}]Cl$_2$ **17**

Pt–P(1)	2.305(1)	P(1)–O(1)	1.582(4)
P(1)–C(1)	1.810(4)	O(1)···Cl(1)	2.957(5)
P(1)–C(11)	1.798(5)	H(1a)···Cl(1)	2.137
C(1)–C(1a)	1.506(9)		
P(1)–Pt–P(1a)	180.0	O(1)–P(1)–C(1)	106.4(2)
P(1)–Pt–P(1b)	84.1(1)	O(1)–P(1)–C(11)	104.8(2)
P(1)–Pt–P(1c)	95.9(1)	C(1)–P(1)–C(11)	103.8(2)
Pt–P(1)–O(1)	111.5(1)	P(1)–C(1)–C(1a)	110.3(3)
Pt–P(1)–C(1)	108.4(1)	O(1)–H(1a)···Cl(1)	162.2
Pt–P(1)–C(11)	120.9(2)	Cl(1s)–C(1s)···Cl(1a)	119.4(9)

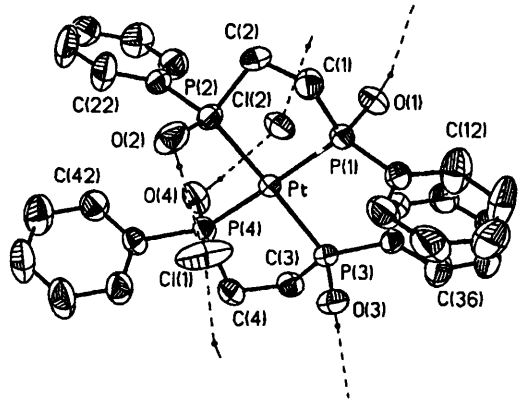

Fig. 7 Molecular structure of *rac*-[Pt{(*RR*,*RR*)- or (*SS*,*SS*)-Ph(OH)P(CH$_2$)$_2$P(OH)Ph}$_2$]Cl$_2$ **18**

Table 7 Bond lengths (Å) and angles (°) for *rac*-[Pt{(*RR*,*SS*)-Ph(OH)P(CH$_2$)$_2$P(OH)Ph}$_2$]Cl$_2$ **18**

Pt–P(1)	2.294(2)	P(2)–C(21)	1.802(6)
Pt–P(2)	2.310(2)	P(3)–C(31)	1.800(6)
Pt–P(3)	2.296(2)	P(4)–C(41)	1.802(6)
Pt–P(4)	2.303(2)	C(1)–C(2)	1.531(8)
P(1)–O(1)	1.579(5)	C(3)–C(4)	1.525(9)
P(2)–O(2)	1.578(6)	Cl(1)···O(2)	2.894(6)
P(3)–O(3)	1.574(5)	Cl(1a)···O(1)	2.956(6)
P(4)–O(4)	1.582(5)	Cl(2)···O(4)	2.953(6)
P(1)–C(1)	1.810(6)	Cl(2a)···O(3)	2.913(6)
P(2)–C(2)	1.809(6)	Cl(1)···H(2o)	2.24(2)
P(3)–C(3)	1.819(6)	Cl(1a)···H(1o)	2.21(2)
P(4)–C(4)	1.812(6)	Cl(2)···H(4o)	2.12(2)
P(1)–C(11)	1.806(6)	Cl(2a)···H(3o)	2.35(2)
P(1)–Pt–P(2)	84.5(1)	O(2)–P(2)–C(2)	105.1(3)
P(3)–Pt–P(4)	84.4(1)	O(3)–P(3)–C(3)	107.5(3)
P(1)–Pt–P(3)	95.1(1)	O(4)–P(4)–C(4)	105.3(3)
P(2)–Pt–P(4)	96.4(1)	O(1)–P(1)–C(11)	106.8(3)
P(2)–Pt–P(3)	174.5(1)	O(2)–P(2)–C(21)	102.8(3)
P(1)–Pt–P(4)	175.6(1)	O(3)–P(3)–C(31)	107.2(3)
Pt–P(1)–O(1)	109.6(2)	O(4)–P(4)–C(41)	102.5(3)
Pt–P(2)–O(2)	112.4(2)	C(1)–P(1)–C(11)	105.4(3)
Pt–P(3)–O(3)	108.5(2)	C(2)–P(2)–C(21)	104.8(3)
Pt–P(4)–O(4)	111.3(2)	C(3)–P(3)–C(31)	104.5(3)
Pt–P(1)–C(1)	107.8(2)	C(4)–P(4)–C(41)	106.0(3)
Pt–P(2)–C(2)	106.6(2)	P(1)–C(1)–C(2)	107.3(4)
Pt–P(3)–C(3)	107.0(2)	P(2)–C(2)–C(1)	109.4(4)
Pt–P(4)–C(4)	108.1(2)	P(3)–C(3)–C(4)	108.8(4)
Pt–P(1)–C(11)	119.4(2)	P(4)–C(4)–C(3)	108.2(4)
Pt–P(2)–C(21)	123.6(2)	P(1)–O(1)–H(1o)	113(6)
Pt–P(3)–C(31)	121.4(2)	P(2)–O(2)–H(2o)	108(7)
Pt–P(4)–C(41)	122.3(2)	P(3)–O(3)–H(3o)	115(6)
O(1)–P(1)–C(1)	107.3(3)	P(4)–O(4)–H(4o)	119(5)

[{Pt[(*RR*,*RR*)-Ph(O)P(CH$_2$)$_2$P(OH)Ph]$_2$}$_n$] and its (*SS*,*SS*) isomer **16**.

Molecular Structures of meso-[{Pt[(*R*,*R*)-Ph(O)P(CH$_2$)$_2$P(OH)Ph][(*S*,*S*)-Ph(O)P(CH$_2$)$_2$P(OH)Ph]}$_n$] **15**, *meso*-[Pt{(*R*,*R*)-Ph(OH)P(CH$_2$)$_2$P(OH)Ph}{(*S*,*S*)-Ph(OH)P(CH$_2$)$_2$P(OH)Ph}]Cl$_2$ **17** *and rac*-[Pt{(*RR*,*RR*)- *or* (*SS*,*SS*)-Ph(OH)P(CH$_2$)$_2$P(OH)Ph}$_2$]Cl$_2$·2CH$_2$Cl$_2$ **18**.—The structures of complexes **15**, **17** and **18** are shown in Figs. 5–7 respectively and selected bond lengths and angles are given in Tables 5–7. The asymmetric unit of **17** consists of one quarter of a dication, one half of a chloride anion and one half of a dichloromethane molecule. Molecules of **15** contain a platinum atom chelated by an (*R*,*R*)- and an (*S*,*S*)-Ph(O)P(CH$_2$)$_2$P(OH)Ph ligand in a square-planar co-ordination geometry (Fig. 5). In contrast to the molecular structure of *syn*-[Pt{(*R*,*S*)-Ph(O)P(CH$_2$)$_2$P(OH)Ph}$_2$] **3** which involves discrete molecules exhibiting intramolecular interligand O–H···O hydrogen bridges, the molecular structure of complex **15** consists of a chain-polymer array constructed from symmetrical intermolecular O···H···O hydrogen bridges. The intermolecular O···O distances of 2.421(10)–2.440(10) Å (Table 5) are indicative of very strong hydrogen bonding.[11] Complex **15** also exhibits interesting phenyl ring packing arrangements. While a regular (eclipsed) stacking of phenyl rings is observed on one side of the chain-polymer array, an alternate or staggered stacking arrangement is observed on the other.

The molecular structure of complex **17** (Fig. 6) exhibits an '*anti*' phosphoryl oxygen configuration required by the co-ordination of the (*R*,*R*) and (*S*,*S*) ligands. This relationship allows each Cl$^-$ ion to participate in hydrogen-bonding interactions with two P–OH groups, one from each ligand [O···Cl distances 2.957(5) Å, Table 6]. The Pt···Cl distances of 3.778(2) and 3.805(2) Å are indicative of non-bonding interactions. The structure of **17** is somewhat reminiscent of the dicationic complex *anti*-[Pt{(*R*,*S*)-Ph(OH)P(CH$_2$)$_2$P(OH)Ph}$_2$]Cl$_2$ **9** (Fig. 3).

The molecular structure of the *rac* complex **18** is shown in Fig. 7. In contrast to complex **17** which exists as discrete molecules, complex **18** in the solid state is a chain-polymer array constructed from intermolecular (P–OH···Cl$^-$···HO–P) hydrogen bonding [O···Cl distances 2.894(6)–2.956(6) Å, Table 7].

Experimental

All operations unless otherwise specified were carried out under an atmosphere of dry N_2 or argon, using dry solvents that were distilled prior to use. Deuteriated solvents were dried over 4 Å molecular sieves and freeze-thawed degassed. Proton NMR spectra were referenced to tetramethylsilane and recorded on a Varian Gemini-300 MHz spectrometer, ^{19}F and ^{31}P-{^{1}H} NMR spectra were obtained on a Gemini-300 MHz spectrometer, and referenced to $CFCl_3$ and 85% H_3PO_4 respectively. Mass spectra were conducted on a VG 70–250S/SE mass spectrometer. Microanalyses were carried out by Canadian Microanalytical Laboratories. Melting points were recorded on a Kofler hot-stage apparatus and are uncorrected. 1,2-Bis(diphenylphosphino)ethane and K_2PtCl_4 were purchased from Digital Specialty Chemicals Inc. Lithium rods and BF_3·Et_2O were purchased from Aldrich. The ligand mixture *meso*- and *rac*-Ph(O)HP(CH$_2$)$_2$PH(O)Ph,[7] and the complexes $SnCl_2Et_2$,[8] [Pt(PPh$_3$)$_4$],[19] and [{PtCl$_2$(C$_2$H$_4$)}$_2$][20] were prepared as reported in the literature.

Purification of the Racemic Ligand (*RR*,*SS*)-Ph(O)HP(CH$_2$)$_2$PH(O)Ph.—To a solid mixture containing the crude ligand Ph(O)HP(CH$_2$)$_2$PH(O)Ph (80% *rac*, 20% *meso*) (5.65 g, 0.020 mol) and $SnCl_2Et_2$ (5.04 g, 0.020 mol) was added CH_2Cl_2 (40 cm^3). The resultant solution was stirred for 1 h at room temperature whereupon a significant amount of white precipitate formed. This solid is composed primarily of a Sn^{IV} complex tentatively formulated as [$SnCl_2Et_2${(*R*,*S*)-Ph(O)HP(CH$_2$)$_2$PH(O)Ph}]. After stirring the mixture overnight, the white solid (2.6 g) was collected on a sintered glass frit and air-dried. The colourless filtrate was made slightly basic by the addition of an aqueous NaOH solution (0.9 mol dm^{-3}, 40 cm^3). At this point, a large amount of a flocculent white precipitate (presumably a Sn^{IV}–hydroxo species) formed. After filtering the mixture and washing the white solid with CH_2Cl_2 (2 × 15 cm^3), the organic layer was separated. The aqueous layer was extracted with fresh CH_2Cl_2 (5 × 30 cm^3) and the combined extracts dried over $MgSO_4$, filtered and concentrated to dryness to afford 3.83 g of 96% pure *rac* ligand (*RR*,*SS*)-Ph(O)HP(CH$_2$)$_2$PH(O)Ph as an off-white solid. The ^{31}P-{^{1}H} NMR spectrum of the ligand in CH_2Cl_2 showed it to be a diastereomeric mixture composed of 96% *rac* and 4% *meso*.

Preparations.—*syn*-[Pt{(*R*,*S*)-Ph(O)P(CH$_2$)$_2$P(OH)Ph}$_2$] **3**. To an orange solution containing [Pt(PPh$_3$)$_4$] (2.233 g, 1.795 mmol) in CH_2Cl_2 (50 cm^3) was added the *meso* ligand (*R*,*S*)-Ph(O)HP(CH$_2$)$_2$PH(O)Ph (0.999 g, 3.590 mmol) as a solid. Gas evolution was observed, and within 5 min the solution was almost colourless. The solution was left to stand overnight and then concentrated to 5–10 cm^3. Addition of hexane (50 cm^3) precipitated the product **3** as a white solid. Recrystallization of the crude product from CH_2Cl_2–hexane afforded **3** (1 g, 77%) as colourless needles, m.p. 235–246 °C (Found: C, 45.0; H, 4.0. $C_{28}H_{30}O_4P_4Pt$ requires C, 44.9; H, 4.0%). ^{31}P-{^{1}H} NMR (CH_2Cl_2): δ 112.9 [s, J(^{195}Pt–^{31}P) 2389 Hz]. Crystals suitable for a single-crystal X-ray diffraction study were obtained by slow evaporation (carried out in air) of a MeOH solution of **3**.

syn-[Pt{(*R*,*S*)-Ph(O)P(CH$_2$)$_2$P(OH)Ph}{(*R*,*S*)-Ph(OH)P(CH$_2$)$_2$P(OH)Ph}]Cl **12**. Hydrogen chloride gas was bubbled slowly through a solution containing *syn*-[Pt{(*R*,*S*)-Ph(O)P(CH$_2$)$_2$P(OH)Ph}$_2$] **3** (0.114 g) in CH_2Cl_2 (3 cm^3) for 1 min.

Table 8 Crystal data, details of intensity measurements and least-squares parameters

	3	**12**	**9**	**13**	**15**	**17**	**18**
Empirical formula	$C_{28}H_{30}O_4P_4Pt$	$C_{28}H_{31}ClO_4P_4Pt$	$C_{28}H_{32}Cl_2O_4P_4Pt$	$C_{29}H_{30}B_2Cl_2F_4O_4P_4Pt$	$C_{28}H_{30}O_4P_4Pt$	$C_{30}H_{36}Cl_6O_4P_4Pt$	$C_{28}H_{32}Cl_2O_4P_4Pt$
Crystal colour, habit	Colourless, needle	Colourless, block	Colourless, block	Colourless, block	Colourless, plate	Colourless, plate	Colourless, needle
Crystal size/mm	0.25 × 0.15 × 0.15	0.20 × 0.25 × 0.15	0.15 × 0.20 × 0.15	0.10 × 0.05 × 0.05	0.25 × 0.20 × 0.02	0.15 × 0.16 × 0.04	0.25 × 0.15 × 0.15
M	749.5	785.9	822.4	930.0	749.5	992.3	822.4
Crystal class	Triclinic	Monoclinic	Monoclinic	Monoclinic	Monoclinic	Monoclinic	Monoclinic
Space group	$P\bar{1}$	$C2/c$	$P2_1/c$	$P2_1/n$	$P2_1/c$	$C2/m$	$P2_1/c$
a/Å	9.942(2)	21.773(4)	10.288(2)	11.434(2)	13.8081(6)	10.529(2)	8.764(1)
b/Å	11.396(2)	8.301(2)	12.926(2)	23.627(8)	16.9147(10)	13.210(2)	24.426(2)
c/Å	26.016(6)	33.516(5)	11.826(2)	13.008(2)	12.3877(8)	14.493(2)	14.290(1)
α/°	101.06(2)	90	90	90	90	90	90
β/°	94.93(2)	93.18(2)	101.51(2)	93.02(2)	104.951(4)	110.64(2)	92.56(1)
γ/°	102.11(2)	90	90	90	90	90	90
U/Å^3	2803.9(14)	6048(3)	1541.0(8)	3509.3(14)	2795.3(3)	1886.4(6)	3056.0(6)
Z	4	8	2	4	4	2	4
D_c/g cm^{-3}	1.755	1.726	1.772	1.760	1.781	1.747	1.787
μ(Mo-Kα)/cm^{-1}	52.66	49.72	49.67	43.88	52.82	43.48	50.09
F(000)	1472	3088	808	1816	1472	976	1616
T/K	294	294	294	294	294	174	294
2θ range/°	3.2 to 45.0	2.4 to 50	3.2 to 45.0	4.6 to 50	4.6 to 50	2.0 to 50	4.4 to 52.6
Octants collected	$\pm h, \pm k, -l$	$h, k, \pm l$	$\pm h, k, l$	$h, k, \pm l$	$-h, k, \pm l$	$\pm h, k, l$	$-h, k, \pm l$
Reflections collected	7599	5885	2297	6731	5404	2681	6900
Unique reflections	7320	5305	2115	6151	4664	2131	6206
Observed reflections [$F > 6.0\sigma(F)$]	5641	3037	1591	3089	3277	2079	3873
Weighting g	0.0004	0.0007	0.0001	0.0008	0.0004	0.0015	0.0004
R	0.028	0.031	0.017	0.038	0.029	0.036	0.027
R'	0.034	0.038	0.024	0.044	0.034	0.048	0.033
Goodness of fit	1.29	0.98	1.24	0.99	1.08	1.01	0.99
Largest Δ/σ	0.23	0.08	0.01	0.01	0.21	0.02	0.03
Parameters refined	684	356	181	416	337	109	369
Δρ(max.), (min.)/e Å^{-3}	0.98, −1.27	0.65, −0.89	0.35, −0.32	1.43, −0.71	0.97, −0.61	1.89, −1.74	0.53, −0.45
Absorption correction	SHELXL[23]	DIFABS[22]	DIFABS[22]	SHELXTL[21]	SHELXTL[21]	DIFABS[22]	SHELXTL[21]
Min., max. absorption corrections	0.326, 0.680	0.918, 1.126	0.887, 1.125	0.377, 0.866	0.305, 0.356	0.809, 1.222	0.515, 0.617

Table 9 Atomic coordinates for *syn*-[Pt{(*R*,*S*)-Ph(O)P(CH_2)$_2$P(OH)Ph}$_2$] **3**

Atom	*x*	*y*	*z*	Atom	*x*	*y*	*z*
Pt(1)	0.416 62(2)	0.228 65(2)	0.131 11(1)	C(26)	0.000 7(8)	−0.003 4(7)	0.113 8(3)
Pt(2)	0.057 26(2)	0.787 75(2)	0.378 82(1)	C(31)	0.565 0(7)	0.534 3(6)	0.121 2(3)
P(1)	0.526 3(2)	0.264 9(2)	0.215 8(1)	C(32)	0.670 1(8)	0.625 4(7)	0.154 0(3)
P(2)	0.281 0(2)	0.056 0(2)	0.149 5(1)	C(33)	0.659 1(10)	0.745 6(7)	0.163 6(3)
P(3)	0.581 6(2)	0.375 9(2)	0.108 3(1)	C(34)	0.544 0(9)	0.776 5(7)	0.142 7(3)
P(4)	0.348 5(2)	0.159 4(2)	0.042 2(1)	C(35)	0.438 6(8)	0.687 2(8)	0.110 2(3)
P(5)	0.190 3(2)	0.969 8(2)	0.368 1(1)	C(36)	0.449 2(7)	0.566 8(7)	0.099 9(3)
P(6)	0.155 8(2)	0.847 4(2)	0.465 6(1)	C(41)	0.219 7(7)	0.233 0(6)	0.016 6(3)
P(7)	−0.119 8(2)	0.645 0(2)	0.397 6(1)	C(42)	0.232 7(8)	0.292 3(7)	−0.025 2(3)
P(8)	−0.065 8(2)	0.751 2(2)	0.296 2(1)	C(43)	0.129 0(9)	0.346 2(8)	−0.041 7(3)
O(1)	0.682 8(5)	0.323 9(4)	0.222 2(2)	C(44)	0.011 8(10)	0.339 4(9)	−0.017 2(4)
O(2)	0.280 9(5)	−0.060 2(4)	0.106 6(2)	C(45)	0.001 3(10)	0.285 0(11)	0.024 2(4)
O(3)	0.729 7(5)	0.378 1(5)	0.135 1(2)	C(46)	0.104 4(9)	0.232 9(9)	0.041 2(4)
O(4)	0.296 4(5)	0.017 8(4)	0.024 1(2)	C(51)	0.365 6(7)	0.965 9(6)	0.355 3(3)
O(5)	0.125 5(5)	1.026 9(4)	0.326 0(2)	C(52)	0.380 9(7)	0.873 4(6)	0.314 6(3)
O(6)	0.048 1(4)	0.831 2(4)	0.505 6(2)	C(53)	0.512 2(9)	0.865 6(8)	0.302 1(3)
O(7)	−0.156 4(4)	0.678 3(4)	0.454 7(2)	C(54)	0.628 7(8)	0.944 8(8)	0.331 0(3)
O(8)	−0.090 3(4)	0.873 5(4)	0.283 1(2)	C(55)	0.613 6(7)	1.034 7(7)	0.372 2(3)
C(1)	0.500 4(8)	0.112 4(6)	0.231 3(3)	C(56)	0.485 1(7)	1.047 0(7)	0.384 1(3)
C(2)	0.351 2(8)	0.039 6(7)	0.214 5(3)	C(61)	0.289 8(7)	0.769 8(6)	0.482 8(3)
C(3)	0.579 2(7)	0.336 9(7)	0.036 6(3)	C(62)	0.406 5(7)	0.776 4(6)	0.456 6(3)
C(4)	0.506 3(7)	0.204 7(6)	0.012 5(3)	C(63)	0.509 2(7)	0.718 6(6)	0.469 2(3)
C(5)	0.245 0(7)	1.010 6(6)	0.477 8(3)	C(64)	0.495 0(7)	0.649 9(6)	0.507 3(3)
C(6)	0.203 4(7)	1.070 2(6)	0.432 8(3)	C(65)	0.376 7(8)	0.638 8(7)	0.533 0(3)
C(7)	−0.270 6(6)	0.644 6(6)	0.351 6(3)	C(66)	0.275 8(7)	0.699 9(6)	0.521 1(3)
C(8)	−0.233 8(6)	0.645 8(6)	0.295 7(3)	C(71)	−0.092 9(6)	0.491 2(6)	0.387 0(3)
C(11)	0.446 7(7)	0.353 2(6)	0.264 8(3)	C(72)	−0.163 6(8)	0.395 9(7)	0.344 8(3)
C(12)	0.427 0(8)	0.326 1(8)	0.314 0(3)	C(73)	−0.127 4(10)	0.283 7(7)	0.337 1(3)
C(13)	0.364 0(10)	0.398 0(10)	0.348 8(4)	C(74)	−0.023 7(9)	0.264 8(8)	0.369 7(3)
C(14)	0.322 4(9)	0.495 5(10)	0.336 8(4)	C(75)	0.045 7(8)	0.356 7(7)	0.411 7(3)
C(15)	0.341 4(9)	0.523 8(7)	0.288 4(4)	C(76)	0.013 1(7)	0.469 9(7)	0.419 7(3)
C(16)	0.403 8(8)	0.452 6(7)	0.252 8(3)	C(81)	0.004 5(6)	0.677 0(6)	0.240 2(3)
C(21)	0.103 0(7)	0.064 5(6)	0.154 0(3)	C(82)	0.010 6(7)	0.553 3(7)	0.231 9(3)
C(22)	0.067 6(9)	0.148 1(7)	0.193 7(3)	C(83)	0.063 3(8)	0.500 9(7)	0.188 2(3)
C(23)	−0.066 3(10)	0.164 1(9)	0.192 1(4)	C(84)	0.113 2(8)	0.571 3(8)	0.153 5(3)
C(24)	−0.165 7(9)	0.098 2(8)	0.151 1(4)	C(85)	0.107 9(8)	0.691 0(8)	0.161 2(3)
C(25)	−0.132 8(8)	0.013 8(8)	0.112 9(4)	C(86)	0.055 3(7)	0.746 6(7)	0.204 1(3)

Hexane (2 cm^3) was slowly added to the resultant white mixture in order to ensure complete precipitation. White needles of **12** were collected, washed with hexane (2 × 3 cm^3) and dried *in vacuo* (0.11 g, 92%), m.p. 170–174 °C. ^{31}P-{^{1}H} NMR (CH_2Cl_2): δ 119.2 [br s, $w^{\frac{1}{2}}$ = 17, J(^{195}Pt–^{31}P) 2465 Hz]. Crystals suitable for a single-crystal X-ray diffraction study were obtained from CH_2Cl_2–ether.

anti-[Pt{(*R*,*S*)-Ph(OH)PCH_2CH_2P(OH)Ph}$_2$]Cl_2 **9**. To a suspension containing [{$PtCl_2(C_2H_4)$}$_2$] (0.202 g, 0.343 mmol) in CH_2Cl_2 (10 cm^3) was added the *meso* ligand (*RS*)-Ph(O)HP(CH_2)$_2$PH(O)Ph (0.383 g, 1.37 mmol) as a solid. The resultant very pale yellow solution was left to stand, and after 5 min a significant amount of small colourless needles formed. After 30 min the colourless needles (fraction 1) were separated from the mother-liquor and air-dried (yield 0.284 g). A ^{31}P-{^{1}H} NMR spectrum of fraction 1 in CH_2Cl_2 showed it to consist of 94% of the monocationic complex **12** and 6% of the desired title complex **9**. The mother-liquor was concentrated to $\frac{1}{4}$ of the original volume whereupon a significant amount of colourless crystals (needles and cubes) formed. The crystals (fraction 2) were collected and air-dried (yield 0.157 g). A ^{31}P-{^{1}H} NMR spectrum of fraction 2 in CH_2Cl_2 showed it to consist of 33% of the monocationic complex **12** and 66% of the desired title complex **9**. An analytical sample of *anti*-[Pt{(*R*,*S*)-Ph(OH)PCH_2CH_2P(OH)Ph}$_2$]Cl_2 **9** was obtained by fractional crystallization from CH_2Cl_2, m.p. > 240 °C (decomp.) (Found: C, 40.9; H, 3.8; P, 15.2. $C_{28}H_{32}Cl_2O_4P_4Pt$ requires C, 40.9; H, 3.9; P, 15.1%). ^{31}P-{^{1}H} NMR (CH_2Cl_2): δ 117.5 [s, J(^{195}Pt–^{31}P) 2587 Hz].

syn-[Pt{[(*R*,*S*)-Ph(O)PCH_2CH_2P(O)Ph]BF_2}$_2$]·CH_2Cl_2 **13**. To a colourless solution containing *syn*-[Pt{(*RS*)-Ph(O)P(CH_2)$_2$P(OH)Ph}$_2$] **3** (0.232 g, 0.309 mmol) in CH_2Cl_2 (10 cm^3) was added BF_3·Et_2O (a total of 1.8 cm^3). The resultant solution was concentrated to 2 cm^3 and diethyl ether (30 cm^3) added. The crude white solid was collected and recrystallized from CH_2Cl_2–Et_2O to give complex **13** as colourless crystals (0.086 g, 33%), m.p. 275–280 °C (Found: C, 37.8; H, 3.3. $C_{28}H_{28}B_2F_4O_4P_4Pt$·$CH_2Cl_2$ requires C, 37.45; H, 3.25%). Mass spectrum (electron impact): *m*/*z* [Pt{[Ph(O)PCH_2CH_2-P(O)Ph]BF_2}$_2$$^+$] 845 (calc.), 845 (found). NMR (CD_2Cl_2): ^{31}P-{^{1}H} δ 119.5 [s, J(^{195}Pt–^{31}P) 2459 Hz]; ^{19}F δ −134.8 [br d, J(^{19}F–^{19}F) 59], −139.1 [br d, J(^{19}F–^{19}F) 60 Hz]. Crystals suitable for a single-crystal X-ray diffraction study were obtained from CH_2Cl_2–Et_2O.

Platinum(II) *complexes containing the racemic ligand.* To a stirred orange solution containing [$Pt(PPh_3)_4$] (0.575 g, 0.462 mmol) in CH_2Cl_2 (15 cm^3) was added 0.257 g (0.988 mmol) of 93% pure *rac* ligand (*RR*,*SS*)-Ph(O)HP(CH_2)$_2$PH(O)Ph. The resultant yellow solution was left to stand, and after 10 min the colour discharged to afford a milky white mixture. After allowing the mixture to stand overnight, the white solid (0.276 g) was collected, washed with CH_2Cl_2 and air-dried. The white solid consists of a mixture of the structurally characterized polymeric complex *meso*-[{Pt[(*RR*)-Ph(O)P(CH_2)$_2$P(OH)-Ph][(*SS*)-Ph(O)P(CH_2)$_2$P(OH)Ph]}$_n$] **15** and presumably *rac*-[{Pt[(*RR*,*SS*)-Ph(O)P(CH_2)$_2$P(OH)Ph]$_2$}$_n$] **16**. While crystals of complex **15** suitable for an X-ray diffraction study were obtained by repeating the above reaction in a layered

Table 10 Atomic coordinates for *syn*-[Pt{(*R*,*S*)-Ph(O)P(CH_2)$_2$P(OH)Ph}{(*R*,*S*)-Ph(OH)P(CH_2)$_2$P(OH)Ph}]Cl **12**

Atom	*x*	*y*	*z*
Pt	0.275 13(1)	0.490 70(4)	0.120 50(1)
P(1)	0.360 0(1)	0.485 2(3)	0.083 2(1)
P(2)	0.219 6(1)	0.484 4(3)	0.060 0(1)
P(3)	0.197 0(1)	0.467 1(3)	0.163 8(1)
P(4)	0.339 8(1)	0.457 8(3)	0.176 3(1)
O(1)	0.409 2(3)	0.358 4(7)	0.097 2(2)
O(2)	0.192 3(4)	0.310 6(9)	0.049 3(2)
O(3)	0.158 8(3)	0.304 3(7)	0.157 4(2)
O(4)	0.396 3(3)	0.352 4(7)	0.170 0(2)
C(1)	0.334 9(5)	0.435 4(11)	0.032 5(3)
C(2)	0.273 4(4)	0.519 9(11)	0.021 3(3)
C(3)	0.232 3(4)	0.454 6(12)	0.214 0(3)
C(4)	0.293 6(4)	0.365 6(11)	0.213 7(3)
C(11)	0.399 3(4)	0.677 0(9)	0.081 6(3)
C(12)	0.462 9(5)	0.680 4(11)	0.087 4(3)
C(13)	0.491 3(5)	0.827 4(15)	0.089 0(3)
C(14)	0.460 4(6)	0.965 4(14)	0.085 9(3)
C(15)	0.396 3(7)	0.963 9(11)	0.081 6(3)
C(16)	0.367 2(5)	0.820 8(10)	0.079 3(3)
C(21)	0.155 2(4)	0.615 9(11)	0.050 3(3)
C(22)	0.105 1(5)	0.572 2(13)	0.025 6(3)
C(23)	0.057 0(5)	0.678 4(15)	0.018 6(3)
C(24)	0.057 6(5)	0.826 0(14)	0.036 7(3)
C(25)	0.107 1(5)	0.871 8(13)	0.060 6(3)
C(26)	0.155 5(5)	0.767 8(12)	0.067 5(3)
C(31)	0.138 4(4)	0.620 0(10)	0.167 0(2)
C(32)	0.077 1(4)	0.581 3(12)	0.166 1(3)
C(33)	0.034 1(5)	0.698 6(13)	0.170 0(3)
C(34)	0.051 5(5)	0.855 5(13)	0.174 2(3)
C(35)	0.111 4(5)	0.897 3(12)	0.174 1(3)
C(36)	0.156 1(4)	0.778 0(11)	0.171 1(3)
C(41)	0.365 4(4)	0.647 1(11)	0.198 2(3)
C(42)	0.349 7(5)	0.793 9(10)	0.179 7(3)
C(43)	0.372 3(5)	0.937 0(12)	0.195 4(3)
C(44)	0.410 4(5)	0.936 2(16)	0.230 1(4)
C(45)	0.423 6(5)	0.793 8(16)	0.248 6(4)
C(46)	0.402 3(4)	0.648 6(14)	0.233 2(3)
Cl	0.241 5(1)	0.090 4(3)	0.113 7(1)

Table 11 Atomic coordinates for *anti*-[Pt{(*R*,*S*)-Ph(OH)P(CH_2)$_2$P(OH)Ph}$_2$]Cl_2 **9**

Atom	*x*	*y*	*z*
Pt	0.0000	0.0000	0.0000
P(1)	−0.0606(1)	0.1646(1)	0.0393(1)
P(2)	0.1870(1)	0.0788(1)	−0.0380(1)
O(1)	0.0005(3)	0.1976(3)	0.1674(3)
O(2)	0.3186(3)	0.0596(3)	0.0557(3)
C(1)	0.0155(4)	0.2468(4)	−0.0533(4)
C(2)	0.1594(4)	0.2185(4)	−0.0413(5)
C(11)	−0.2296(4)	0.2084(3)	0.0170(4)
C(12)	−0.3145(5)	0.1910(4)	−0.0874(4)
C(13)	−0.4412(5)	0.2314(4)	−0.1060(5)
C(14)	−0.4812(5)	0.2887(4)	−0.0224(6)
C(15)	−0.3983(5)	0.3053(5)	0.0809(5)
C(16)	−0.2727(5)	0.2657(4)	0.1004(4)
C(21)	0.2340(4)	0.0439(3)	−0.1710(4)
C(22)	0.3590(4)	0.0104(4)	−0.1753(4)
C(23)	0.3924(6)	−0.0126(4)	−0.2801(5)
C(24)	0.3016(6)	−0.0045(4)	−0.3789(5)
C(25)	0.1763(6)	0.0252(4)	−0.3761(5)
C(26)	0.1409(5)	0.0484(4)	−0.2725(5)
Cl	0.2166(1)	0.0547(1)	0.2740(1)

solvent mixture consisting of MeOH and CH_2Cl_2, the existence of the *rac* complex **16** is inferred from the preparation of the dicationic Pt^{II} complexes shown below.

Dicationic complexes meso-[Pt{(*R*,*R*)-Ph(OH)PCH_2CH_2P(OH)Ph}{(*S*,*S*)-Ph(OH)PCH_2CH_2P(OH)Ph}]Cl_2 **17** *and rac*-[Pt{(*RR*,*RR*)- *or* (*SS*,*SS*)-Ph(OH)PCH_2CH_2P(OH)Ph}$_2$]

Table 12 Atomic coordinates for *syn*-[Pt{[(*R*,*S*)-Ph(O)P(CH_2)$_2$P(O)Ph]BF_2}$_2$]-CH_2Cl_2 **13**

Atom	*x*	*y*	*z*
Pt	0.195 53(4)	0.169 43(2)	0.390 40(3)
P(1)	0.053 6(3)	0.190 8(1)	0.265 3(2)
P(2)	0.066 3(3)	0.186 0(1)	0.516 3(2)
P(3)	0.324 0(3)	0.178 9(1)	0.263 2(2)
P(4)	0.338 8(3)	0.177 1(1)	0.518 2(2)
O(1)	−0.016 3(7)	0.244 1(3)	0.298 5(6)
O(2)	−0.012 9(7)	0.237 9(3)	0.487 5(6)
O(3)	0.452 6(6)	0.207 5(3)	0.484 9(6)
O(4)	0.446 0(7)	0.206 1(3)	0.295 6(6)
F(1)	−0.115 7(7)	0.304 9(4)	0.396 3(6)
F(2)	0.082 8(8)	0.308 8(3)	0.402 9(7)
F(3)	0.533 8(7)	0.132 2(3)	0.392 6(6)
F(4)	0.617 5(6)	0.220 1(3)	0.391 1(6)
B(1)	0.516 4(14)	0.190 2(7)	0.394 7(13)
B(2)	−0.013 4(14)	0.276 3(6)	0.397 8(11)
C(1)	0.129 1(10)	0.209 7(5)	0.147 6(8)
C(2)	0.253 8(10)	0.230 4(5)	0.174 6(8)
C(3)	0.153 6(9)	0.203 5(5)	0.634 7(8)
C(4)	0.275 3(10)	0.225 5(5)	0.608 7(9)
C(11)	−0.055 9(10)	0.138 3(5)	0.228 1(9)
C(12)	−0.027 8(12)	0.092 1(6)	0.171 5(10)
C(13)	−0.109 2(15)	0.050 9(7)	0.149 2(13)
C(14)	−0.219 5(17)	0.055 4(8)	0.181 9(13)
C(15)	−0.247 9(15)	0.102 9(8)	0.237 5(12)
C(16)	−0.168 9(12)	0.144 7(6)	0.261 1(10)
C(21)	−0.036 3(11)	0.130 7(5)	0.551 0(9)
C(22)	0.007 4(14)	0.081 1(6)	0.589 7(10)
C(23)	−0.070 2(17)	0.039 0(7)	0.616 5(12)
C(24)	−0.185 1(19)	0.047 5(9)	0.605 6(12)
C(25)	−0.231 5(15)	0.097 0(8)	0.567 7(13)
C(26)	−0.155 7(12)	0.139 9(6)	0.539 4(9)
C(31)	0.344 0(10)	0.117 1(5)	0.185 7(8)
C(32)	0.412 8(14)	0.119 6(6)	0.102 8(10)
C(33)	0.419 6(18)	0.073 4(9)	0.038 9(13)
C(34)	0.358 5(19)	0.025 2(8)	0.056 2(12)
C(35)	0.288 6(12)	0.023 3(7)	0.138 2(13)
C(36)	0.283 8(11)	0.069 0(5)	0.204 5(10)
C(41)	0.382 8(9)	0.114 1(5)	0.588 2(8)
C(42)	0.451 0(12)	0.118 5(6)	0.679 0(9)
C(43)	0.489 4(14)	0.070 3(7)	0.728 5(10)
C(44)	0.460 1(12)	0.018 0(6)	0.691 6(10)
C(45)	0.393 5(14)	0.013 1(6)	0.603 2(12)
C(46)	0.356 2(13)	0.061 3(6)	0.552 9(11)
Cl(1)	0.342 6(9)	0.359 6(4)	0.392 0(8)
Cl(2)	0.586 9(8)	0.390 9(3)	0.394 9(5)
C(1s)	0.476 5(19)	0.348 3(9)	0.364 9(20)

Cl_2 **18**. To a suspension of the white solid (0.26 g) containing the polymeric complex *meso*-[{Pt[(*R*,*R*)-Ph(O)P(CH_2)$_2$P(OH)Ph][(*S*,*S*)-Ph(O)P(CH_2)$_2$P(OH)Ph]}$_n$] **15** and presumably *rac*-[{Pt[(*RR*,*RR*)- or (*SS*,*SS*)-Ph(O)P(CH_2)$_2$P(OH)Ph]$_2$}$_n$] **16** in CH_2Cl_2 (5 cm^3) was added dry HCl for 2 min. After analysing the resultant clear and colourless solution by ^{31}P-{^1H} NMR spectroscopy, a layer of diethyl ether (5 cm^3) was added to the solution and the two-phase system allowed to stand overnight. Crystals of *meso*-[Pt{(*R*,*R*)-Ph(OH)P(CH_2)$_2$P(OH)Ph}{(*S*,*S*)-Ph(OH)P(CH_2)$_2$P(OH)Ph}]Cl_2 **17** and *rac*-[Pt{(*RR*,*RR*)- or (*SS*,*SS*)-Ph(OH)PCH_2CH_2P(OH)Ph}$_2$]Cl_2 **18** formed (combined yield 0.21 g), and each complex was subjected to a single-crystal X-ray diffraction study.

Relative Rate Studies into the Decomposition of the Intermediate Platinum(IV) trans-*dihydride Complex syn*-[PtH_2{(*R*,*S*)-Ph(O)P(CH_2)$_2$P(OH)Ph}$_2$] **4** *to the Thermodynamic Complex syn*-[Pt{(*R*,*S*)-Ph(O)P(CH_2)$_2$P(OH)Ph}$_2$] **3**.—In each of two separate experiments [$Pt(PPh_3)_4$] (0.134 g, 0.108 mmol) and the *meso* ligand (*R*,*S*)-Ph(O)HP(CH_2)$_2$PH(O)Ph (0.060 g, 0.215 mmol) were dissolved in CD_2Cl_2 (0.8 cm^3). The

Table 13 Atomic coordinates for *meso*-[{Pt[(*R*,*R*)-Ph(O)P(CH$_2$)$_2$P(OH)Ph][(*S*,*S*)-Ph(O)P(CH$_2$)$_2$P(OH)Ph]}$_n$] **15**

Atom	*x*	*y*	*z*
Pt(1)	0.121 51(2)	0.242 43(1)	0.135 92(2)
P(1)	0.038 8(1)	0.350 2(1)	0.184 2(2)
P(3)	0.032 0(1)	0.148 8(1)	0.204 9(2)
P(2)	0.220 7(1)	0.334 2(1)	0.079 8(1)
P(4)	0.196 6(1)	0.137 9(1)	0.069 1(2)
O(1)	0.053 3(4)	0.366 3(3)	0.309 6(4)
O(2)	0.205 1(3)	0.347 7(3)	−0.046 8(4)
O(3)	0.035 3(3)	0.151 9(3)	0.331 0(4)
O(4)	0.211 5(3)	0.144 6(3)	−0.050 3(4)
C(1)	0.082 8(5)	0.436 0(4)	0.123 1(6)
C(2)	0.198 6(5)	0.428 1(3)	0.143 4(6)
C(3)	0.079 6(5)	0.051 9(3)	0.178 4(6)
C(4)	0.112 8(5)	0.053 8(3)	0.069 1(6)
C(11)	−0.094 9(5)	0.357 4(3)	0.121 6(6)
C(12)	−0.133 3(6)	0.353 6(4)	0.005 6(6)
C(13)	−0.233 9(6)	0.364 4(4)	−0.038 2(7)
C(14)	−0.296 7(6)	0.376 5(5)	0.028 7(8)
C(15)	−0.259 8(6)	0.380 4(5)	0.142 6(8)
C(16)	−0.159 5(6)	0.369 7(4)	0.189 1(7)
C(21)	0.351 1(5)	0.312 2(3)	0.139 3(6)
C(22)	0.388 5(6)	0.308 2(4)	0.254 6(7)
C(23)	0.486 6(7)	0.284 1(5)	0.298 2(7)
C(24)	0.546 5(6)	0.263 7(5)	0.231 1(8)
C(25)	0.510 0(6)	0.268 0(5)	0.120 1(8)
C(26)	0.412 8(6)	0.291 5(4)	0.071 5(7)
C(31)	−0.099 0(5)	0.142 4(3)	0.132 8(6)
C(32)	−0.132 4(6)	0.158 9(4)	0.018 8(6)
C(33)	−0.230 8(6)	0.149 4(4)	−0.035 6(7)
C(34)	−0.298 7(6)	0.124 0(5)	0.019 3(8)
C(35)	−0.267 4(7)	0.108 5(5)	0.130 1(9)
C(36)	−0.168 1(6)	0.116 9(4)	0.187 7(7)
C(41)	0.315 0(5)	0.101 1(3)	0.154 6(6)
C(42)	0.337 1(5)	0.101 8(4)	0.270 3(6)
C(43)	0.423 8(6)	0.065 0(5)	0.332 2(8)
C(44)	0.486 9(6)	0.028 0(5)	0.281 3(9)
C(45)	0.467 4(6)	0.029 6(5)	0.166 5(9)
C(46)	0.382 4(5)	0.065 0(4)	0.102 7(7)

Table 14 Atomic coordinates for *meso*-[Pt{(*R*,*R*)-Ph(OH)P(CH$_2$)$_2$P(OH)Ph}{(*S*,*S*)-Ph(OH)P(CH$_2$)$_2$P(OH)Ph}]Cl$_2$ **17**

Atom	*x*	*y*	*z*
Pt	0.0000	0.0000	0.0000
P(1)	0.1121(1)	0.1296(1)	0.1030(1)
O(1)	0.2620(3)	0.1422(3)	0.1040(3)
C(1)	0.0252(5)	0.2471(3)	0.0555(3)
C(11)	0.1286(6)	0.1305(3)	0.2308(3)
C(12)	0.0127(7)	0.1261(5)	0.2540(4)
C(13)	0.0233(10)	0.1321(6)	0.3521(5)
C(14)	0.1470(10)	0.1395(6)	0.4254(5)
C(15)	0.2622(9)	0.1426(6)	0.4032(4)
C(16)	0.2552(7)	0.1392(5)	0.3045(4)
Cl(1)	0.2974(2)	0.0000	−0.0426(1)
C(1s)	0.5593(9)	0.0000	0.2327(6)
Cl(1s)	0.6249(2)	0.1094(1)	0.2988(1)

resultant colourless solutions were then subjected to different conditions (part 1: no change, 'blank run'; part 2: 2 drops of D_2O added) and the progress of each reaction monitored by ^1H and ^{31}P-{^1H} NMR spectroscopy. In another experiment, part 3, [Pt(PPh$_3$)$_4$] (0.131 g, 0.105 mmol) and the *meso* ligand (*R*,*S*)-Ph(O)HP(CH$_2$)$_2$PH(O)Ph (0.058 g, 0.210 mmol) were dissolved in CD_2Cl_2 (1 cm^3). Hydrogen chloride gas was bubbled through the resultant colourless solution for 2 min and the progress of the reaction monitored by ^1H and ^{31}P-{^1H} NMR spectroscopy.

Crystal Structure Determinations.—Intensity data for compounds **3**, **9**, **12**, **13**, **15** and **18** were collected on an Enraf-

Table 15 Atomic coordinates for *rac*-[Pt{(*RR*,*SS*)-Ph(OH)P(CH$_2$)$_2$P(OH)Ph}$_2$]Cl$_2$ **18**

Atom	*x*	*y*	*z*
Pt	0.210 03(3)	0.206 15(1)	0.487 30(1)
P(1)	0.355 6(2)	0.272 2(1)	0.562 6(1)
P(2)	0.385 5(2)	0.146 0(1)	0.555 2(1)
P(3)	0.051 3(2)	0.266 9(1)	0.408 2(1)
P(4)	0.050 6(2)	0.140 6(1)	0.420 6(1)
O(1)	0.273 5(5)	0.292 1(2)	0.652 7(3)
O(2)	0.504 4(7)	0.124 9(2)	0.483 7(4)
O(3)	0.131 3(6)	0.286 2(2)	0.317 4(3)
O(4)	−0.059 9(6)	0.116 2(2)	0.494 5(3)
C(1)	0.534 7(7)	0.241 0(2)	0.601 8(4)
C(2)	0.497 3(7)	0.184 7(3)	0.641 8(4)
C(3)	−0.120 0(6)	0.229 4(2)	0.371 0(4)
C(4)	−0.073 4(7)	0.173 8(3)	0.332 9(4)
C(11)	0.407 7(7)	0.332 9(2)	0.499 5(4)
C(12)	0.370 7(9)	0.383 6(3)	0.530 9(6)
C(13)	0.412 2(11)	0.429 3(3)	0.481 2(7)
C(14)	0.491 4(11)	0.424 8(3)	0.404 0(6)
C(15)	0.533 2(11)	0.374 8(3)	0.373 3(5)
C(16)	0.490 8(9)	0.328 3(3)	0.419 6(4)
C(21)	0.333 5(7)	0.084 2(2)	0.614 8(4)
C(22)	0.412 6(9)	0.036 5(3)	0.601 2(5)
C(23)	0.373 5(11)	−0.010 6(3)	0.647 2(6)
C(24)	0.261 8(10)	−0.010 0(3)	0.708 8(5)
C(25)	0.184 5(9)	0.037 2(3)	0.724 3(5)
C(26)	0.222 1(8)	0.084 4(3)	0.677 8(5)
C(31)	−0.018 6(6)	0.327 3(2)	0.464 4(4)
C(32)	−0.096 7(7)	0.323 2(3)	0.545 6(4)
C(33)	−0.158 9(9)	0.368 9(3)	0.586 2(5)
C(34)	−0.138 7(11)	0.419 4(3)	0.544 8(6)
C(35)	−0.060 5(11)	0.424 0(3)	0.464 4(6)
C(36)	−0.000 3(9)	0.378 2(3)	0.423 6(5)
C(41)	0.122 1(7)	0.080 0(2)	0.365 6(4)
C(42)	0.134 2(8)	0.032 0(3)	0.416 1(5)
C(43)	0.186 0(9)	−0.015 0(3)	0.374 6(6)
C(44)	0.224 8(10)	−0.013 9(3)	0.283 6(6)
C(45)	0.215 8(10)	0.032 9(3)	0.233 3(5)
C(46)	0.165 0(8)	0.080 3(3)	0.273 5(5)
Cl(1)	0.501 3(2)	0.178 8(1)	0.303 3(1)
Cl(2)	−0.093 5(2)	0.184 3(1)	0.663 2(1)
H(1o)	0.328 4(87)	0.305 6(33)	0.689 5(54)
H(2o)	0.487 5(97)	0.137 1(33)	0.441 9(50)
H(3o)	0.086 3(77)	0.293 2(28)	0.284 2(46)
H(4o)	−0.080 7(85)	0.135 5(31)	0.541 0(50)

Nonius CAD-4 diffractometer at 294 K using graphite-monochromated Mo-Kα radiation (λ = 0.710 73 Å). Intensity data for compound **17** were collected on a Siemens diffractometer at 174 K using graphite-monochromated Mo-Kα radiation (λ = 0.710 73 Å). The ω scan technique was applied with variable scan speeds. Intensities of three standard reflections measured every 2 h, for each crystal, showed negligible variation. For all compounds the heavy-atom positions were solved by Patterson methods and the locations of all non-hydrogen atoms were determined from subsequent Fourier-difference syntheses. In each case all non-hydrogen atoms were refined with anisotropic thermal parameters by full-matrix least squares to minimize $\Sigma w(F_o - F_c)^2$, where $w^{-1} = \sigma^2(F_o) + gF_o^2$. Hydrogen atoms bonded to carbon atoms were positioned on geometric grounds (C–H 0.96 Å) and included in the refinement as riding atoms with general thermal parameters for each structure [0.063(3) **3**, 0.068(4) **9**, 0.062(6) **12**, 0.095(9) **13**, 0.065(4) **15**, 0.046(7) **17** and 0.074(4) Å^2 **18**]. The hydrogen atoms bonded to oxygen in structures **12** and **18** were refined with isotropic thermal parameters. In the remaining structures, the hydroxyl hydrogen-atom positions were identified from Fourier-difference maps and then included in the refinement in calculated positions with refined isotropic thermal parameters. Crystal data, data collection, and least-squares parameters are listed in Table 8. All calculations were performed using

SHELXTL PC[21] on a 486-66 personal computer. Relevant bond lengths and angles are given in Tables 1–7 and atomic coordinates in Tables 9–15.

Additional material available from the Cambridge Crystallographic Data Centre comprises H-atom coordinates, thermal parameters and remaining bond lengths and angles.

Acknowledgements

We thank the Natural Sciences and Engineering Research Council of Canada for financial support.

References

1 D. M. Roundhill, R. P. Sperline and W. B. Beaulieu, *Coord. Chem. Rev.*, 1978, **26**, 263.
2 H. Alper and M. Sommovigo, *Tetrahedron Lett.*, 1993, 59.
3 P. Leoni, F. Marchetti and M. Pasquali, *J. Organomet. Chem.*, 1993, **451**, C25.
4 P. W. N. M. van Leeuwen, C. F. Roobeek and J. H. G. Frijns, *Organometallics*, 1990, **9**, 1211.
5 H. Goldwhite, *Introduction to Phosphorus Chemistry*, Cambridge University Press, Cambridge, 1981, pp. 306–308.
6 V. I. Nefedov, Y. V. Salyn, B. Walther, B. Messbauer and R. Schops, *Inorg. Chim. Acta*, 1980, **45**, L103.
7 (*a*) K. Issleib, *Z. Chem.*, 1979, **19**, 417; (*b*) P. Brooks, D. C. Craig, M. J. Gallagher, A. D. Rae and A. Sarroff, *J. Organomet. Chem.*, 1987, **323**, C1.
8 O. H. Johnson, H. E. Fritz, D. A. Halvorson and R. L. Evans, *J. Am. Chem. Soc.*, 1955, **77**, 5857.
9 L. E. Godycki and R. E. Rundle, *Acta Crystallogr.*, 1953, **6**, 487.
10 P. Gilli, V. Bertolasi, V. Ferretti and G. Gilli, *J. Am. Chem. Soc.*, 1994, **116**, 909.
11 D. V. Naik, G. J. Palenik, S. Jacobson and A. J. Carty, *J. Am. Chem. Soc.*, 1974, **96**, 2286.
12 D. W. W. Anderson, E. A. V. Ebsworth and D. W. H. Rankin, *J. Chem. Soc., Dalton Trans.*, 1973, 854.
13 J. Chatt and B. L. Shaw, *J. Chem. Soc.*, 1962, 5075.
14 A. J. Lough, S. Park, R. Ramachandran and R. H. Morris, *J. Am. Chem. Soc.*, 1994, **116**, 8365.
15 W. C. Hamilton and J. A. Ibers, *Hydrogen Bonding in Solids*, W. A. Benjamin, New York, 1968, p. 16.
16 W. B. Beaulieu, T. B. Rauchfuss and D. M. Roundhill, *Inorg. Chem.*, 1975, **14**, 1732.
17 K. R. Dixon and A. D. Rattray, *Inorg. Chem.*, 1977, **16**, 209.
18 R. Bartsch, S. Hietkamp, S. Morton, H. Peters and O. Stelzer, *Inorg. Chem.*, 1983, **22**, 3624.
19 R. Ugo, F. Cariatti and G. La Monica, *Inorg. Synth.*, 1968, **11**, 105.
20 J. Chatt and M. L. Searle, *Inorg. Synth.*, 1957, **5**, 210.
21 G. M. Sheldrick, SHELXTL PC, Siemens Analytical X-Ray Instruments Inc., Madison, WI, 1990.
22 N. Walker and D. Stuart, *Acta Crystallogr., Sect. A*, 1983, **39**, 158.
23 G. M. Sheldrick, SHELXL 93, University of Göttingen, 1993.

Received 14*th March* 1995; *Paper* 5/01641J